Swarm and Evolutionary Computation 48 (2019) 62–71

Contents lists available at ScienceDirect

Swarm and Evolutionary Computation

journal homepage: www.elsevier.com/locate/swevo

A novel scalable test problem suite for multimodal multiobjective optimization

Caitong Yue [a], Boyang Qu [b], Kunjie Yu [a], Jing Liang [a,*], Xiaodong Li [c]

[a] School of Electrical Engineering, Zhengzhou University, Zhengzhou, 450001, China
[b] School of Electronic and Information Engineering, Zhongyuan University of Technology, Zhengzhou, 450007, China
[c] School of Science, Computer Science and Information Technology, RMIT University, Melbourne, 3000, Australia

ARTICLE INFO

Keywords:
Multimodal
Multiobjective
Test problem suite
Benchmark functions

ABSTRACT

This paper proposes a novel scalable multimodal multiobjective test problem suite. The proposed test problems have various properties, such as presence of local Pareto optimal set (PS), scalable number of PSs, nonuniformly distributed PSs, discrete Pareto front (PF), and scalable number of variables and objectives. All of the test problems proposed in this paper are continuous optimization problems. Therefore, they can be used to measure different capacities of multimodal multiobjective continuous optimization algorithms. Moreover, a landscape visualization method for multiobjective problems is proposed to show the properties of the multimodal multiobjective test problems. Based on the landscapes, the characteristics of these problems are analyzed and characterized. Furthermore, the existing multimodal multiobjective optimization algorithms and several popular multiobjective algorithms are tested and compared with the novel test problem suite. Then, a discussion on the desired properties of multimodal multiobjective optimization algorithms and future works on multimodal multiobjective optimization are presented.

1. Introduction

In real-world applications, many optimization problems are "multimodal", that is, they have multiple satisfactory solutions. The traditional multimodal optimization [1–6] problem refers to a single objective problem with multiple global/local peaks. In fact, many multiobjective optimization problems are also "multimodal". To be specific, there are multiple global or local Pareto optimal sets (PSs) in some real-world multiobjective problems, which are called multimodal multiobjective optimization (MMO) problems [7–10].

It is of significant importance to find multiple PSs of MMO problems. The first reason is that different PSs may be suitable for different decision makers. Second, providing multiple PSs helps reveal the potential properties of the problems. Third, shifting from one PS to another helps solve dynamic optimization problems [11]. Fourth, offering multiple PSs increases the probability of finding robust solutions. However, the study of MMO is still in the emerging stage. Although many real-word applications [12,13] are actually MMO problems, to date the researchers have not investigated them in depth.

Fortunately, there are several pioneering studies on MMO. Deb proposed MMO problems in Ref. [7], but no special algorithm is designed to solve this kind of problems. Later, he designed the Omni-optimizer [14] aiming to solve different types of problems, including uni/multimodal single/multiobjective problems. The Omni-optimizer performs much better than the original NSGAII [15]. Rudolph et al. [16] analyzed the capabilities of evolutionary multiobjective algorithms to maintain multiple Pareto subsets and designed the SYM-PART test problem. Ishibuchi et al. proposed multimodal multiobjective test problems for visually examining diversity maintenance behavior in the decision space [17,18]. Although the number of objectives is scalable in these test problems, the number of decision variables is fixed to two. Subsequently, Ishibuchi et al. [19] and Masuda et al. [20] proposed multimodal multiobjective test problems with scalable number of decision variables. Recently, Liang et al. [9] proposed two MMO test problems and designed DN-NSGAII to solve them. Further, Yue et al. [8] designed six more MMO test problems and proposed MO_Ring_PSO_SCD to solve these problems. In addition, they developed a novel performance indicator *PSP* to compare the performance of different algorithms on MMO problems. Subsequently, some new algorithms for MMO were proposed. Liu et al. [21] proposed a double-niched evolutionary algorithm and analyzed its behavior on

* Corresponding author.
E-mail addresses: zzuyuecaitong@163.com (C. Yue), qby1984@hotmail.com (B. Qu), yukunjie@zzu.edu.cn (K. Yu), liangjing@zzu.edu.cn (J. Liang), xiaodong.li@rmit.edu.au (X. Li).

https://doi.org/10.1016/j.swevo.2019.03.011
Received 13 August 2018; Received in revised form 16 March 2019; Accepted 20 March 2019
Available online 28 March 2019

polygon-based problems. Tanabe et al. [22] proposed a decomposition-based evolutionary algorithm for MMO. Liu et al. [23] proposed a multimodal multiobjective evolutionary algorithm using two-archive and recombination strategies and designed several novel multimodal multiobjective test problems.

Since many researchers are becoming interested in MMO [7–10,14,16,24,25], there is definitely a need for designing MMO benchmark test problems to assess and compare the effectiveness of the newly developed MMO algorithms. Benchmark test problems are of great significance for the developing optimization algorithms [26]. First, test functions test an algorithm's capacity to tackle a certain aspect of real-world problems. Second, they can be used to compare several algorithms systematically. Third, they may help to understand the working principles of different algorithms. Fourth, they inspire the development of novel algorithms.

Several MMO test problems have been proposed in the past decades. Rudolph et al. [16] designed the SYM-PART test problem with a controllable number of PSs. However, SYM-PART heavily relies on symmetry properties of the underlying single objective functions. In addition, the number of its variables and objectives are unscalable. Deb et al. [14] designed the Omni-test function which has $3n$ (n is the number of variables) PSs corresponding to the same PF. Although both the numbers of variables and of PS are both scalable, the number of objectives is fixed. In Ref. [9], Liang et al. proposed two simple multimodal multiobjective test problems—SS-UF1 and S-UF3. They are modified from unimodal multiobjective test problems by symmetry and shift. Subsequently, Liang's research team designed six more test problems [8]. However they still have several shortcomings: (*i*) the number of PSs is fixed; (*ii*) the dimensions of variables and objectives are low and unscalable; (*iii*) only global PSs are known, and their local PSs are complex and unknown.

Test problems are desired to test algorithms' ability to deal with a special aspect of real-world problems. Therefore, a benchmark test problem suite should include different types of characteristics of real-word problems. As for MMO, the test problem suite is desired to have the following properties:

1) Coexistence of global PSs and local PSs;
2) Controllable number of PSs;
3) Various PSs shapes;
4) All the PSs are known;
5) Scalable number of variables;
6) Scalable number of objectives.

Based on the above considerations, a novel MMO benchmark test problem suite is designed in this paper. The difficulty of each proposed test problem is controllable and they can be used to test different aspects of MMO algorithms. The main contributions of this paper are listed as follows:

1) Three different frameworks to generate MMO test problems are presented.
2) A test problem suite containing twenty-three test problems is established.
3) A way to visualize the landscape of MMO test problems is proposed.
4) The characteristics of all the test problems in the test suite are analyzed based on their landscapes.
5) The existing MMO algorithms and several most popular multiobjective algorithms are tested on the novel benchmark test problem suite.

2. Related definitions

There are different definitions about domination, global/local PS and global/local PF [7–10,23,27]. In this paper, the definitions are in line with those in Refs. [7–9,23], which are familiar to the researchers in the field of evolutionary computation.

Given a multiobjective optimization problem Min $\vec{f}(\vec{x}) = [f_1(\vec{x}), f_2(\vec{x}), \ldots, f_m(\vec{x})]$, a feasible solution $\vec{x_1}$ is said to dominate the other feasible $\vec{x_2}$ if both of the following conditions are met [7]:

1) The solution $\vec{x_1}$ is no worse than $\vec{x_2}$ for all objectives, i.e. $f_i(\vec{x_1}) \leq f_i(\vec{x_2})$ for $i = 1, \ldots, m$;
2) The solution $\vec{x_1}$ is strictly better than $\vec{x_2}$ for at least one objective, i.e. $f_i(\vec{x_1}) < f_i(\vec{x_2})$ for $i \in [1, m]$.

A solution is called a *nondominated* solution if it is not dominated by any other solution. All *nondominated* solutions constitute a Pareto optimal set (PS). The set of all the vectors in the objective space that corresponds to the PS is called the Pareto front (PF).

The local PS, PF and global PS, PF [7] are defined as follows:

Local Pareto optimal set (Local PS): For an arbitrary member $\vec{x}$ in a solution set P_L, if there exists no neighborhood solution $\vec{y}$ satisfying $\|\vec{y} - \vec{x}\|_\infty \leq \sigma$ (σ is a small positive value), dominating any member in set P_L, then the solution set P_L is defined as the local PS;

Global Pareto optimal set (Global PS): For an arbitrary member in a solution set P_G, there exists no solution in the feasible space dominating any member in the set P_G, then the solution set P_G is defined as the global PS.

Local Pareto Front (Local PF): The set of all the vectors in the objective space that corresponds to the local PS is defined as the local Pareto Front.

Global Pareto Front (Global PF): The set of all the vectors in the objective space that corresponds to the global PS is defined as the global Pareto Front.

Fig. 1 shows a bi-objective minimization problem with one local PS and one global PS. Solid lines along with stars represent the global PS/PF, while dashed lines with circled dots represent the local PS/PF. Although the local PF is dominated by the global PF, it dominates individuals in its neighborhood as defined above. Note that a certain multimodal multiobjective problem may have several local PSs and global PSs.

A multiobjective optimization problem is an MMO problem if it meets one of the following conditions:

1) It has at least one local Pareto optimal solution;
2) It has at least two global Pareto optimal solutions corresponding to the same point on the PF.

The local Pareto optimal solution [22] represents the solution that is not dominated by any neighborhood solution. The global Pareto optimal solution [22] is not dominated by any solutions in the feasible space.

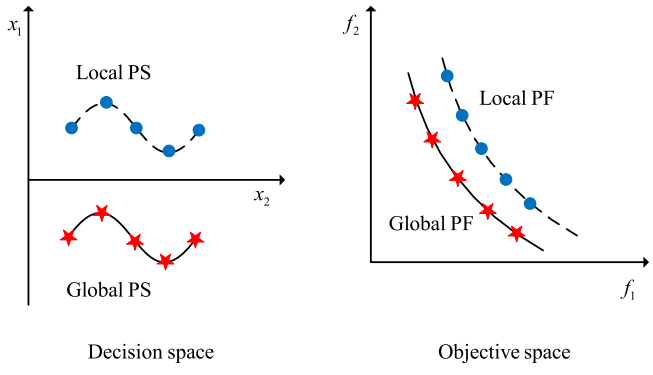

Fig. 1. Illustration of local PS, global PS, local PF and global PF.

3. Design approaches and desired characteristics of MMO test problems

3.1. Design approach

Two main approaches are used to design MMO test problems. The first generates from unimodal multiobjective problems, while the second generates from multimodal single objective problems. Unimodal multiobjective problems are multiobjective problems with only one global PS and without any local PS. Multimodal single objective problems refer to single objective problems with multiple global or local peaks. An introduction to these two methods is presented in the following texts.

3.1.1. Generating MMO test problems from unimodal multiobjective problems

MMO problems can be generated from unimodal multiobjective problems through copying PS by shift or symmetry transformation [8,9]. This is an intuitive way to reproduce several PSs to formulate MMO problems. Fig. 2 illustrates the method to copy PS by shift or symmetry transformation. The continuous line represents the original PS termed PS_1, PS_2 is generated by shift and PS_3 is generated by symmetry transformation. The main advantage of this approach is that it is simple and intuitive. Moreover, the derived MMO problems through this approach inherit all the PF characteristics of the original test problem. If this method is applied to existing unimodal multiobjective test problems, a large number of MMO test problems will be created. However, this approach has two disadvantages. First, all the reproduced PSs are of the same shape. Second, the derived MMO problems have only global PF because all the reproduced PSs correspond to the same PF.

3.1.2. Generating MMO test problems from multimodal single objective problems

Another way to design MMO problems is embedding multimodal single objective problems [28,29] as one component of the MMO problem, that is used in Refs. [7,26,27,30]. The modality of the reproduced MMO problems is controlled by the multimodal single objective problems. To describe this method clearly, a simple bi-objective optimization problem with two variables is taken as an example.

The bi-objective optimization problem is shown in Eq. (1).

$$\text{Min}\begin{cases} f_1(x_1,x_2) = x_1 \\ f_2(x_1,x_2) = \dfrac{g(x_2)}{x_1} \end{cases} \tag{1}$$

where $x_1 > 0$, $g(x_2) > 0$ is a function of x_2 only. In the objective space, f_1 and f_2 have the following relationship: $f_1(x_1,x_2)\cdot f_2(x_1,x_2) = g(x_2)$. If there is only one x_2^* meeting $g(x_2^*) \le g(x_2)$, i.e. $g(x_2)$ is a unimodal function of x_2, the bi-objective optimization problem described in Eq. (1) has only one PF $f_1(x_1,x_2)\cdot f_2(x_1,x_2) = g(x_2^*)$. Therefore it is a unimodal bi-objective optimization problem. However, if $g(x_2)$ is a multimodal function of x_2, for example $g(x_2)$ has two optima $g(x_2^{1*})$ and $g(x_2^{2*})$, the bi-objective optimization problem described in (1) has two PFs: PF1 $f_1(x_1,x_2)\cdot f_2(x_1,x_2) = g(x_2^{1*})$, and PF2 $f_1(x_1,x_2)\cdot f_2(x_1,x_2) = g(x_2^{2*})$. Thus, it turns into a multimodal bi-objective optimization problem.

The advantage of this approach is its flexibility. It can reproduce both local and global PSs of different shapes.

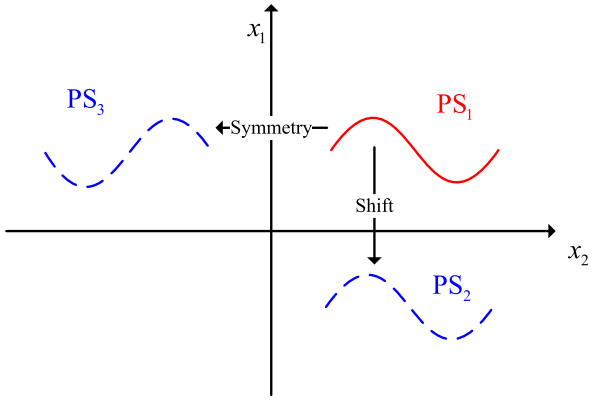

Fig. 2. Copy PS by shift or symmetry transformation.

3.2. Desired characteristics of MMO test problems

The constructed test problems should include multiple characteristics to assess special aspects of the multiobjective optimization evolutionary algorithm (MOEA). Furthermore, it can be used to evaluate the capability of an MOEA to solve problems with a certain number of characteristics, that is the robustness of an MOEA. Table 1 presents eight desired characteristics of MMO test problems as well as comments on the characteristics.

These characteristics are described in the following.

Characteristic 1: Scalable number of variables

It is beneficial if the number of variables is scalable. As the number of variable increases, the dimension of decision space becomes higher. Therefore, this characteristic enables the problem to test the ability of an MOEA to solve problems with different number of variables.

Characteristic 2: Scalable number of objectives

The test problems are expected to have a scalable number of objectives since the number of objectives influences the difficulty of test problems [31]. As the number of objectives increase, it is difficult to have enough convergence strength to the true PF. Hence, this characteristic tests the convergence strength of an MOEA.

Characteristic 3: Pareto optima known

The true PS and PF are expected to be known enabling the measures and analysis of results. Many performance indicators require information of the true PS and PF. Therefore, knowing the location of the PS and PF is necessary to evaluate the performance of a given MOEA accurately.

Characteristic 4: Pareto front geometry

This characteristic tests the capacity of an MOEA dealing with different PF shapes. PF geometry includes convex/concave, linear/nonlinear, continuous/discontinuous and so on. Some algorithms prefer convex PF, while others may do well with concave PF. Generally, a nonlinear PF is more difficult to be found than a linear PF. As for the problem with disconnected PF, some algorithms may fail to find all regions of the PF. In multiobjective problems with three or more objectives, the shape of the PF is important as well as the curvature property. This is because the performance of some well-known evolutionary multiobjective algorithms depends on the shape of the PF [32].

Characteristic 5: Pareto set geometry

Diverse types of PS geometry are necessary to test an MOEA's ability

Table 1
Desired characteristics of MMO test problems.

Characteristic (C)	Comment
C1: Scalable number of variables	Increases flexibility, demands scalability
C2: Scalable number of objectives	Increases flexibility, demands scalability
C3: Pareto optima known	Facilitates the use of measures, analysis of results, in addition to other benefits
C4: Pareto front geometry	Convex/concave, linear/nonlinear, connected/disconnected, or some combination
C5: Pareto set geometry	Linear/nonlinear, connected/disconnected, symmetric/nonsymmetric
C6: Scalable number of Pareto set	Increases flexibility, demands scalability
C7: Coexistence of global and local Pareto set	Encourages EAs to jump out of local optima

to find different types of PS. The PS geometry can be linear/nonlinear, connected/disconnected, symmetric/nonsymmetric and other complex shapes. Some evolutionary multiobjective algorithms may perform well only on particular PS shapes.

Characteristic 6: Scalable number of Pareto set

One important characteristic of MMO test problems is that they have a scalable number of Pareto sets (including the number of global and local PSs). Generally speaking, test problems with more PSs need more computational resources and they may be more difficult to solve.

Characteristic 7: Coexistence of global and local Pareto set

An MMO test problem is expected to have both global and local PS. Some algorithms may fall into local PS. Therefore, test problems with this characteristic can test the global search ability of a certain algorithm.

4. MMO test problem generation frameworks

To generate MMO test problems with different characteristics, three frameworks are presented. Their properties, advantages, and disadvantages are analyzed in detail.

4.1. Framework 1

The design begins with a simple two-objective optimization test problem framework with only two variables:

$$\text{Min}\begin{cases} f_1(x_1,x_2)=x_1 \\ f_2(x_1,x_2)=\dfrac{g(x_2)}{x_1} \end{cases} \tag{2}$$

where $x_1>0,\ \ g(x_2)>0$ and g is a multimodal function. In objective space, f_1 and f_2 have special relationship: $f_1\cdot f_2=g(x_2)$.

The framework described in Eq. (2) has two intuitive yet useful properties:

1) It has a local or global Pareto optimal solution $x_2=x_2^*$, where x_2^* is the local or global optimum of g(x), and x_1 is arbitrary in its range.
2) Its PF is a hyperbola ($f_1\cdot f_2=g(x_2^*)$).

Based on the above properties, different types of MMO test problems can be constructed by changing the type of function g. The PSs and PFs are easy to comprehended. The number of local or global PSs is easily controlled by function g.

However, the framework has some shortcomings. First, the number of objectives and variables are limited to two. Second, the shape of the PF is fixed as a continuous hyperbola.

4.2. Framework 2

In real-world applications, some of the PFs are discontinuous. Hence, a test problem framework with discontinuous PF is constructed.

$$\text{Min}\quad \begin{cases} f_1(\overrightarrow{x})=f_1(x_1,\ x_2,\ldots,\ x_m) \\ f_2(\overrightarrow{x})=g(x_{m+1},\ x_{m+2},\ldots,\ x_N)\cdot h(f_1,\ g) \end{cases} \tag{3}$$

where g is a multimodal function, and h is a monotonically nondecreasing function in g for a fixed value of f_1 and a monotonically decreasing function of f_1 for a fixed value of g.

Framework 2 has three advantages. First, the dimension of variable space is tunable. Second, the distribution (uniform or nonuniform) and diversity in the PF change with different types of function f_1. Third, the convexity and discontinuity of the PF are affected by function h. However, the dimension of objective is fixed.

4.3. Framework 3

The objective number of both Framework 1 and Framework 2 is fixed to two. Therefore, a framework with a scalable number of objective and variables is presented.

$$\text{Min}\quad \begin{cases} f_1(\overrightarrow{x})=f_1(x_1) \\ f_2(\overrightarrow{x})=f_2(x_2) \\ \vdots \\ f_{M-1}(\overrightarrow{x})=f_{M-1}(x_{M-1}) \\ f_M(\overrightarrow{x})=g(x_M)\cdot h(f_1(x_1),\ f_2(x_2),\ \ldots\ , \\ \quad f_{M-1}(x_{M-1}),\ \ g(x_M)) \end{cases} \tag{4}$$

where g and h have the same requirement as Framework 2.

The Framework 3 has three advantages. First, the dimension of both variable and objective space is tunable. Second, the distribution (uniform or nonuniform) and diversity in the PF changes with different types of function f_1. Third, the convexity or discontinuity of the PF can be controlled by function h.

Any number of MMO test problems can be generated using these above three frameworks. In this paper, twelve novel test problems are designed, which have representative characteristics enabling researchers to test various aspects of different MMO algorithms. An MMO test problem suite containing twenty-three test problems is established. Eleven of them have been used in our previous work [8]. The details, including problem equations, search space, true global PS/PF and local PS/PF of these test problems, are in the attached Appendix.

Table 2 lists the characteristics of these MMO test problems. The first column lists the name of the problems, while the top row shows the characteristic names. In the table, '✓' represents that the test problem has the corresponding characteristic, while, '×' means it does not. It is concluded that the MMO test problems have various characteristics. The novel test problems have more desired characteristics than the previous ones. There are many real-world problems similar to the proposed test problems, such as the location selection optimization problem in Ref. [18], job shop scheduling problem, feature selection problem and drug molecule design problem in Ref. [33]. Therefore, the test problem suite can test an algorithm's capacity to tackle a certain aspect of real-world problems. Some of the real-world problems will be modeled and included in a future MMO test problem suite.

5. Visualizing the landscape of MMO test problems

The motivations to visualize the landscape of multiobjective test problems are listed as follows:

1) Checking if the test problems are correctly designed;
2) Showing the properties of test problems intuitively;
3) Promoting the design of algorithms to solve these test problems.

In evolutionary multiobjective optimization, it is very meaningful and useful to visualize the distribution in both the decision space and objective space. Prior researchers have proposed several methods for landscape visualization [34,35]. Fonseca [36] discussed the visualization of trade-off data from single and multiple runs in multiobjective and constrained optimization. Tusar et al. [37] presented a review of visualization methods in the objective space. However, they neglected visualization in the decision space. An interesting and excellent way to visualize the landscapes of MMO problems is proposed in Ref. [38]. However, gradients of some points for the problems MMF2-6 do not exist and the threshold to determine local efficient set varies for different problems. Researchers are encouraged to develop a novel visualization method based on [38] after addressing the above issues.

In this paper, the nondomination rank values are used to visualize the landscape of multiobjective test problems. The most popular method to compare two solutions in multiobjective problems is the nondominated sorting scheme. This scheme ranks all the feasible solutions according to their nondomination level based on their objective function values. As shown in Fig. 3, the nondomination rank value of the first front is 1, of the

Table 2
Characteristics of the MMO test problem suite.

MMO test problem name	C1: Scalable number of variables	C2: Scalable number of objectives	C3: Pareto optima known	C4: PF geometry	C5: PS geometry	C6: Scalable number of PS	C7: Coexistence of global and local PS
SYM-PART simple	×	×	✓	Convex	Linear	×	×
SYM-PART rotated	×	×	✓	Convex	Linear	×	×
Omni-test	✓	×	✓	Convex	Linear	✓	×
MMF1	×	×	✓	Convex	Nonlinear	×	×
MMF1_z	×	×	✓	Convex	Nonlinear	×	×
MMF1_e	×	×	✓	Convex	Nonlinear	×	×
MMF2	×	×	✓	Convex	Nonlinear	×	✓
MMF3	×	×	✓	Convex	Nonlinear	×	✓
MMF4	×	×	✓	Concave	Nonlinear	×	×
MMF5	×	×	✓	Convex	Nonlinear	×	×
MMF6	×	×	✓	Convex	Nonlinear	×	×
MMF7	×	×	✓	Convex	Nonlinear	×	×
MMF8	×	×	✓	Concave	Nonlinear	×	×
MMF9	×	×	✓	Convex	Linear	✓	×
MMF9_r	×	×	✓	Convex	Linear, Rotation	✓	×
MMF10	×	×	✓	Convex	Linear	×	✓
MMF11	×	×	✓	Convex	Linear	✓	✓
MMF12	×	×	✓	Convex, Discontinuous	Linear	✓	✓
MMF13	×	×	✓	Convex	Nonlinear	✓	✓
MMF14	✓	✓	✓	Concave	Linear	✓	×
MMF14_a	✓	✓	✓	Concave	Nonlinear	✓	×
MMF15	✓	✓	✓	Concave	Linear	✓	✓
MMF15_a	✓	✓	✓	Concave	Nonlinear	✓	✓

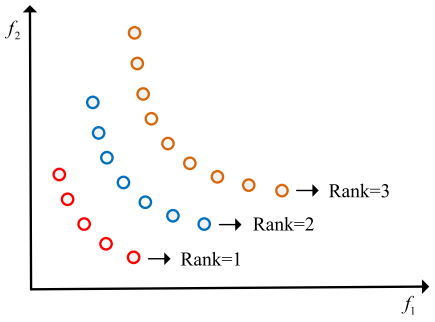

Fig. 3. Nondomination rank.

second front is 2 and so forth. The solutions with lower (better) rank are preferred.

The procedure of visualizing the landscape of MMO problems are described as follows.

Step 1: A population is uniformly generated (uniformly-spaced sampling)[1] in its feasible space.
Step 2: The population is evaluated using its objective functions.
Step 3: Rank value is assigned to each individual using nondomination sorting scheme.
Step 4: The landscape is visualized using rank values.

Fig. 4 shows the landscape of the above MMO test problems. With the help of the visualization method, the size and shape of basins are shown intuitively. As shown in Fig. 4 (m) and (n), although both MMF10 and MMF11 have one global and one local PS, their properties are quite different. The two basins of MMF11 are of similar shape and size, while MMF10 has one narrow basin and one wide basin. MMF12 has many basins since its PS is composed of discontinuous pieces. In Fig. 4 (p), it is clear that the PSs of MMF13 are nonlinear. All the characteristics shown in Fig. 4 are coincident with the description in Section 4 and the Appendix, which verifies that these MMO test problems are designed correctly. Note that if the dimension of decision space is higher than two, it is difficult to visualize the landscape directly. One way to deal with this issue is by choosing one or two dimensions in which the decision maker is interested. For example, for MM13, the landscape in x_2 and x_3 is given in Fig. 4 (p).

The proposed visualization method has several advantages and disadvantages. It has three advantages: (*i*) The gradients of the problems are not required. (*ii*) It is easy to implement since the nondomination sorting scheme is commonly used. (*iii*) It directly displays the dominance relations in the decision space. The disadvantages are: (*i*) It can only show the landscape in two dimensions. (*ii*) It does not work well on many-objective problems because most of the solutions are nondominated in the many-objective situation. Some issues remain for future research, such as visualizing the landscape using high dimensional visualization technology, visualizing the search process of evolutionary algorithms, and developing a general landscape visualization method.

6. Experimental results of different algorithms

In this section, five algorithms, including three MMO algorithms and two popular multiobjective optimization algorithms NSGAII and SPEA2, are tested on the proposed test problems.

MO_Ring_PSO_SCD was proposed by Yue et al. [8]. It uses ring topology to restrict the communication among the population aiming to form stable niches. In this way, different PSs can be detected. In environmental selection, MO_Ring_PSO_SCD uses the nondomination level and special crowding distance to maintain multiple PSs. With the help of these two operators, MO_Ring_PSO_SCD performs well on MMO problems.

DN-NSGAII [9] was modified from NSGAII. It embeds a niching technique in mating selection and environmental selection scheme. Since crowding distance in decision space is used, DN-NSGAII can obtain good distribution in the decision space.

Omni-optimizer [14] was proposed by Deb aiming to solve different types of optimization problems including single objective,

[1] The term "uniformly generated in its feasible space" means uniformly-spaced sampling in the decision space. To be specific, if 10,000 points need to be generated in the two-dimension decision space, the decision space is divided into a grid of 100 by 100 evenly.

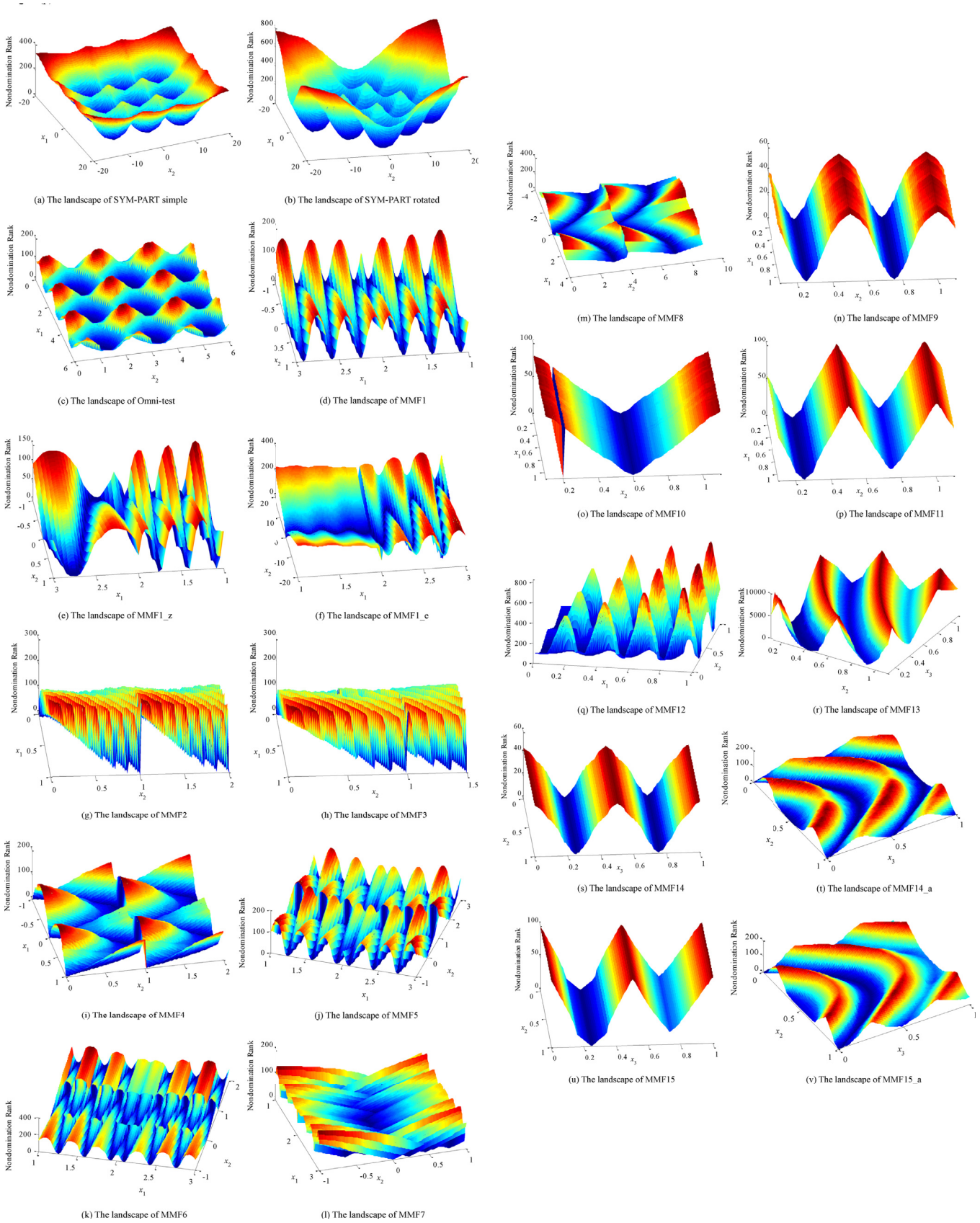

Fig. 4. The landscape of proposed MMO test problems.

multiobjective, unimodal, and multimodal problems. The main procedure of the Omni-optimizer is similar to that of NSGAII [15]. However, the environmental selection criterion of the Omni-optimizer is different from that of NSGAII. In NSGAII, the crowding distance in objective space is used while crowding distances in both objective space and decision space are used to select better solutions. This selection scheme enables it to solve different types of optimization problems.

6.1. Comparisons of the performance indicators of different algorithms

Four performance indicators, Pareto Sets Proximity (*PSP*) [8], Inverted Generational Distance (*IGD* [39]) in decision space (*IGDX*) [40], Hypervolume (*HV*) [41], and *IGD* in objective space (*IGDF*) [40] are used to compare the performance of the five algorithms. Among the indicators, *PSP* and *IGDX* are used to compare the performance in the decision space, while *HV* and *IGDF* are used to compare the performance in the objective space. As for *PSP* and *HV*, the larger value means the better performance, while for *IGDX* and *IGDF*, the smaller means the better. In this paper, 1/*PSP* and 1/*HV* are used instead of *PSP* and *HV* so that for all the four indicators the smaller value means the better performance. For fair comparison, the population size is set to 100**N_var* and the maximal evaluation is set to 5000**N_var*, where *N_var* is the number of variables. For each problem, 21 independent runs are carried out. The results of MMF9-15 are displayed in Fig. 5. To provide comprehensive results, the indicators and statistical test results of the four new test problems are listed in Table 3. The obtained PSs and PFs of median 1/*PSP* run are plotted in Figs. A13–36 of the appendix.

In Fig. 5, each column corresponds to one of the four performance indicators (in all the boxplots, the smaller value means the better performance), and each row corresponds to one of the seven test problems. Within each boxplot, the corresponding indicators of the five optimization algorithms across the 21 runs are plotted. The numerals on the horizontal axis of each plot indicate the following algorithms: 1: MO_Ring_PSO_SCD, 2: Omni-optimizer, 3: DN-NSGAII, 4: NSGAII, and 5: SPEA2. It can be concluded that MO_Ring_PSO_SCD performs best on MMF11-MMF15 according to 1/*PSP* and *IGDX* values. As for MMF9-10, the performances of MO_Ring_PSO_SCD and Omni-optimizer are comparative. The 1/*PSP* and *IGDX* values of DN-NSGAII and Omni-optimizer are similar to each other on MMF9-MMF15. In conclusion, MO_Ring_PSO_SCD, Omni-optimizer and DN-NSGAII perform better in the decision space, because these three algorithms employ the crowding distance in the decision space for environmental selection. As for 1/*HV* and *IGDF*, NSGAII has the best performance on MMF9. For the other test problems, the performance in the objective space is not obvious.

In Table 3, the best results (the smallest values) are in bold words. It can be concluded that MO_Ring_PSO_SCD performs the best on all the four test problems according to 1/*PSP* and *IGDX* and it has a statistically significant difference with the other algorithms. Therefore, MO_Ring_PSO_SCD achieves the best performance in the decision space. The reason is that ring topology and special crowding distance all help to promote the performance in the decision space. As for the objective space, NSGAII, Omni-optimizer and DN-NSGAII perform better than the others according to 1/*HV* because they use the crowding distance in the objective space as the second environmental selection criterion. However, if judging from *IGDF*, MO_Ring_PSO_SCD performs the best on three test problems, because special crowding distance takes advantage of the crowding distance in the objective space. For the remaining algorithms, their performance in the objective space is almost equivalent. In the decision space, DN-NSGAII performs a little better than the other two algorithms. The Wilcoxon's rank sum test is employed to determine whether the best result has a statistically significant difference from the others, and the null hypothesis is rejected at the significance level of 5%. The values of h are included in Table 3 where $h = 1$ means there is a statistically significant difference between the current result and the best one; while $h = 0$ means there is no statistically significant difference between them. It can be concluded that MO_Ring_PSO_SCD has a statistically significant difference from the others according to 1/*PSP* and *IGDX*. As for 1/*HV* and *IGDF*, Omni-optimizer, DN-NSGAII and NSGAII are similar to each other.

Figs. A13–36 show whether global/local PSs/PFs are found. MMF9 has two global PSs. It tests whether the algorithms can detect and maintain all the global PSs simultaneously. In Figs. A13, A15 and A16, MO_Ring_PSO_SCD finds most parts of the two PSs, while SPEA2 only finds one of the PSs. It may be owing to the strong convergence of SPEA2. For DN-NSGAII, Omni-optimizer and NSGAII, only parts of the PSs are found while the others are missing. In Fig. A14, most of the algorithms lose the PS on the right part, because it is enlarged. In Fig. A17, Omni-optimizer finds only the local PS since MMF10 has a wide local basin and a narrow global basin. SPEA2 can find almost the whole global PS, while DN-NSGAII and NSGAII find parts of global PS and parts of local PS. For MO_Ring_PSO_SCD only a few nondominated solutions are found. In fact, the solutions in the local basin are more robust than those in the global one. Therefore, both of the PSs need to be found for further selection. In Figs. A18–19, none of these algorithms can find local PSs of MMF11 and MMF12. In Figs. A20–24, the performances of these algorithms deteriorate markedly when the dimensionality of decision space increases. In Figs. A25–36, if parts of the local/global PSs are missing, the corresponding parts of the local/global PF are also missing in objective space.

6.2. Convergence behavior of different algorithms

The convergence behaviors of these algorithms are analyzed on two typical MMO test problems MMF9 and MMF10. MM9 has n_p (in this section, n_p is set to 2 for convenience's sake) global PSs while MMF10 has one global PS and one local PS. As shown in Fig. 4 (l)-(m), all the global PSs of MMF9 are of the same basin size while the local PS of MMF10 has a larger basin size than its global one. The search space of MMF9 and MMF10 is divided into two subregions, namely Region 1 $\{x_1 \in [0.1,\ 1.1],\ x_2 \in [0.1,\ 0.6]\}$ and Region 2 $\{x_1 \in [0.1,\ 1.1],\ x_2 \in (0.6,\ 1.1]\}$. There is one global/local PS in each subregion. The convergence behaviors of the algorithms are presented by the proportion of individuals in Region 1 for each generation (the proportion of individuals in Region 2 can be also represented by that of Region 1, because the sum of them is 1). Ideally, the proportion in Region 1 should converge to 50% if the algorithm performs well on MMF9. As for MMF10, if the algorithm is trapped in the local PS, the proportion in Region 2 will be larger than in Region 1 since the local PS of MMF10 is in Region 2. If the algorithm can maintain only global Pareto optimal solutions, the proportion in Region 1 will be larger than in Region 2. If the algorithm can maintain both global and local Pareto optimal solutions, the proportion in each subregion will converge to 50%. Therefore, MMF9 can test the algorithm's capacity to maintain several global PS, while MMF10 can test its preference for global or local PS. These five algorithms are tested on both MMF9 and MMF10 for 21 independent times. The maximal generation is set to 100 and the other parameters are the same as in Section 6.1. The mean proportions of 21 runs are shown in Fig. 6.

Fig. 6 shows the convergence behaviors of different algorithms. The continuous line represents the ideal proportion in Region 1 which is equal to 0.5, and the dotted lines of different types represent the proportion in Region 1 of different algorithms. Fig. 6 (a) shows that the proportion in Region 1 is approaching 50% for MO_Ring_PSO_SCD, Omni-optimizer, DN-NSGAII, and NSGAII. For SPEA2, the proportion in Region 1 is smaller than 0.5, which indicates that most individuals of SPEA2 converge to Region 2. Fig. 6 (b) shows that the proportions in Region 1 are much larger than 0.5 for Omni-optimizer, DN-NSGAII, NSGAII and SPEA2. The reason is that the global PS is located in Region 1. It can be concluded that the four algorithms converge to the global PS but miss the local one. Only MO_Ring_PSO_SCD maintains almost equal proportions in the two regions. In many real-world problems, the global PS is so difficult to realize that the local PS is desired actually [33].

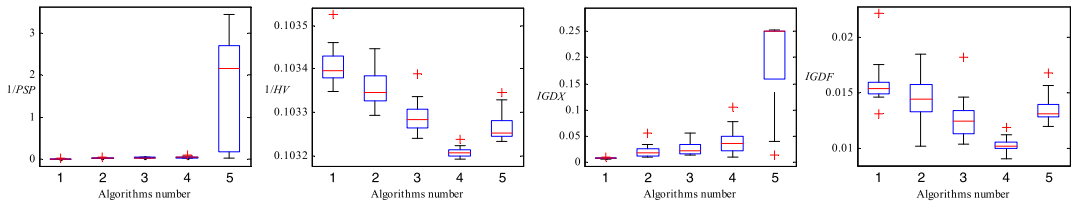

(a) Results on MMF9

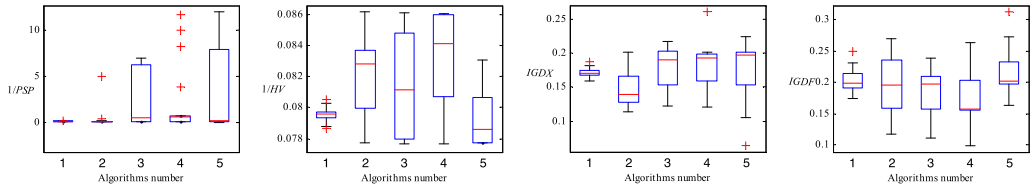

(b) Results on MMF10

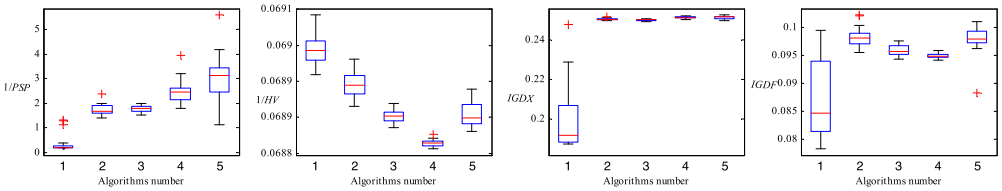

(c) Results on MMF11

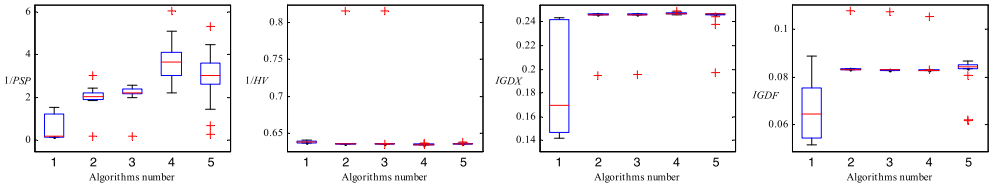

(d) Results on MMF12

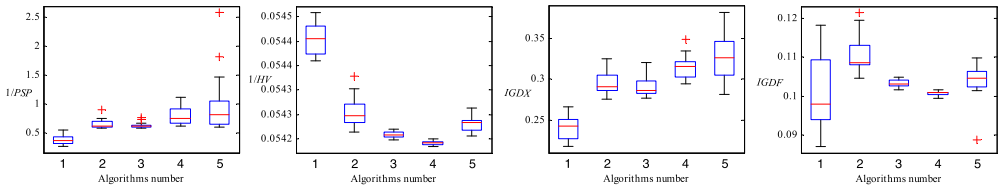

(e) Results on MMF13

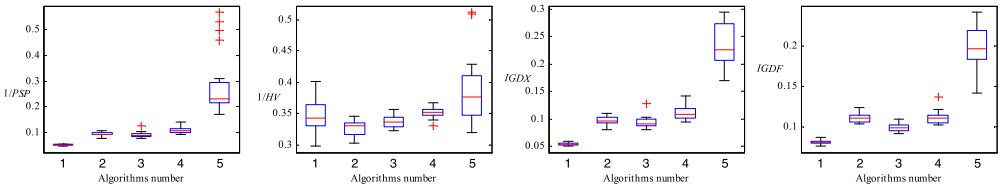

(f) Results on MMF14

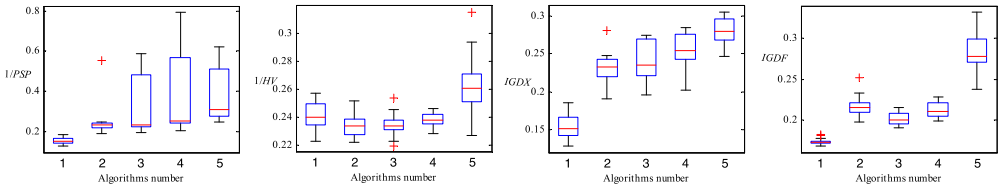

(g) Results on MMF15

Fig. 5. The indicators of different algorithms on seven test problems. The numerals on the horizontal axis of each plot indicate the following algorithms: 1: MO_Ring_PSO_SCD, 2: Omni-optimizer, 3: DN-NSGAII, 4: NSGAII, and 5: SPEA2.

Table 3
The comparison results of different algorithms (mean ± std (*h*)).

Function	Indicator (Ideal value[a])	MO_Ring_PSO_SCD	DN-NSGAII	Omni-optimizer	NSGAII	SPEA2
MMF1_z	1/*PSP* (0)	**0.0354 ± 0.0016**	0.0760 ± 0.0137 (1)	0.0798 ± 0.0174 (1)	0.1717 ± 0.0922 (1)	0.5142 ± 0.4180 (1)
	1/*HV* (1.1443)	1.1485 ± 5.5037e-04 (1)	1.1484 ± 0.011 (1)	1.1473 ± 0.0013 (0)	**1.1470 ± 0.0013**	1.2241 ± 0.0644 (1)
	IGDX (0)	**0.0352 ± 0.0016**	0.0748 ± 0.0134 (1)	0.0777 ± 0.0162 (1)	0.1593 ± 0.0607 (1)	0.3363 ± 0.1469 (1)
	IGDF (0)	0.0036 ± 1.6489e-04 (1)	0.0035 ± 3.3205e-04 (1)	0.0032 ± 4.0659e-04 (1)	**0.0030 ± 4.2398 e-04**	0.0525 ± 0.0550 (1)
MMF1_e	1/*PSP* (0)	**0.5677 ± 0.1331**	1.7492 ± 0.9283 (1)	1.9950 ± 1.3681 (1)	2.3813 ± 2.1201 (1)	11.3950 ± 8.3396 (1)
	1/*HV* (1.1443)	1.1998 ± 0.0354 (1)	1.4169 ± 0.4493 (1)	1.1834 ± 0.0306 (0)	**1.1691 ± 0.0131**	1.1935 ± 0.0272 (1)
	IGDX (0)	**0.4905 ± 0.0866**	1.1981 ± 0.4644 (1)	1.2674 ± 0.5601 (1)	1.3481 ± 0.6216 (1)	2.7373 ± 0.8399 (1)
	IGDF (0)	**0.0126 ± 0.0019**	0.0248 ± 0.0189 (0)	0.0241 ± 0.0217 (0)	0.0149 ± 0.0090 (0)	0.0318 ± 0.0178 (1)
MMF9_r	1/*PSP* (0)	**0.0067 ± 4.1000e-04**	0.0134 ± 0.0137 (1)	0.0106 ± 0.0074 (1)	0.0262 ± 0.0102 (1)	0.0212 ± 0.0218 (1)
	1/*HV* (1.7910)	0.5449 ± 2.2818e-04 (1)	0.5469 ± 0.0035 (1)	0.5437 ± 4.1459e-05 (1)	**0.5437 ± 2.9658e-05**	0.5440 ± 1.8799e-04 (1)
	IGDX (0)	**0.0067 ± 3.9580e-04**	0.0127 ± 0.0123 (1)	0.0100 ± 0.0064 (1)	0.0242 ± 0.0083 (1)	0.0194 ± 0.0173 (1)
	IGDF (0)	0.0032 ± 1.5763e-04 (1)	0.0023 ± 9.2090e-05 (1)	**0.0021 ± 9.2519e-05**	0.0022 ± 1.0084e-04 (0)	0.0027 ± 1.8059e-04 (1)
MMF14_a	1/*PSP* (0)	**0.0599 ± 0.0018**	0.1188 ± 0.0.0077 (1)	0.1102 ± 0.0078 (1)	0.1318 ± 0.0106 (1)	0.2749 ± 0.1387 (1)
	1/*HV* (0.2458)	0.3314 ± 0.0264 (0)	**0.3235 ± 0.0163**	0.3275 ± 0.0094 (0)	0.3492 ± 0.0056 (1)	0.3976 ± 0.0507 (1)
	IGDX (0)	**0.0598 ± 0.0018**	0.1188 ± 0.0077 (1)	0.1102 ± 0.0078 (1)	0.1315 ± 0.0106 (1)	0.2270 ± 0.0686 (1)
	IGDF (0)	**0.0783 ± 0.0020**	0.1199 ± 0.0072 (1)	0.1044 ± 0.0046 (1)	0.1192 ± 0.0074 (1)	0.2160 ± 0.0268 (1)
MMF15_a	1/*PSP* (0)	**0.1643 ± 0.0106**	0.2178 ± 0.0312 (1)	0.2608 ± 0.0320 (1)	0.2686 ± 0.0326 (1)	0.2663 ± 0.0351 (1)
	1/*HV* (0.1881)	0.2396 ± 0.0112 (1)	0.2319 ± 0.0127 (0)	**0.2289 ± 0.0055**	0.2352 ± 0.0050 (1)	0.2732 ± 0.0318 (1)
	IGDX (0)	**0.1620 ± 0.0098**	0.2092 ± 0.0169 (1)	0.2210 ± 0.0138 (1)	0.2321 ± 0.0084 (1)	0.2347 ± 0.0136 (1)
	IGDF (0)	**0.1741 ± 0.0027**	0.2207 ± 0.0087 (1)	0.2077 ± 0.0075 (1)	0.2145 ± 0.0093 (1)	0.2908 ± 0.0235 (1)

[a] Ideal value is the indicator value of the reference solution set. The reference data are available on http://www5.zzu.edu.cn/ecilab/Benchmark/Multimodal_Opt.htm.

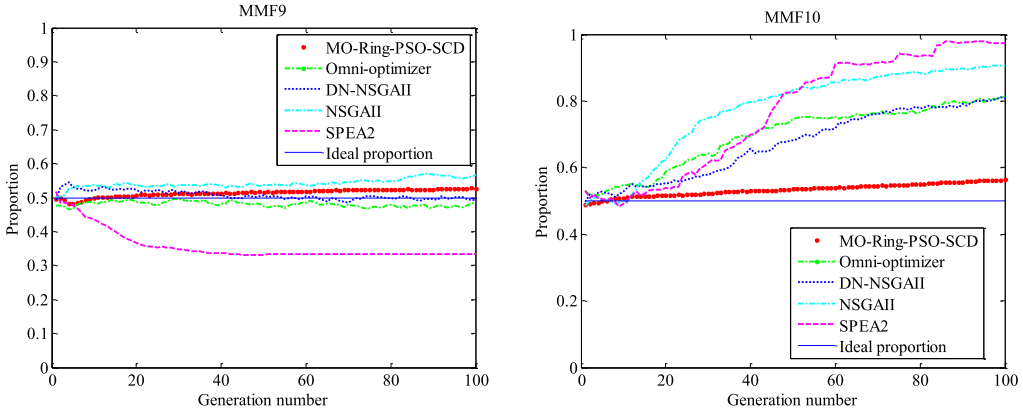

(a) The proportion of individuals in Region 1 on MMF9 (b) The proportion of individuals in Region 1 on MMF10

Fig. 6. The convergence behaviors of different algorithms.

Therefore, algorithms that can find both global and local PS need to be proposed in the future. In addition, how to choose one local PS if a problem possesses multiple local PSs and how to choose one solution in local or global PS are also challenges in MMO.

7. Conclusions

A novel multimodal multiobjective optimization (MMO) test problem suite is proposed in this paper. First, three different frameworks are presented to guide the design of MMO test problems. Based on these frameworks, twelve novel MMO test problems with different characteristics are generated. They can be used to test various aspects of MMO algorithms. Furthermore, a landscape visualization method of a multiobjective optimization problem is provided to check whether the test problems are designed correctly and to show the property of multiobjective problems intuitively. Finally, both MMO algorithms and popular multiobjective optimization algorithms are tested on these problems. From the experimental results and convergence behaviors analysis, it can be concluded that traditional multiobjective optimization algorithms can only maintain parts of PSs while MMO algorithm can find more Pareto optimal solutions. Although, the tested MMO algorithms can obtain most parts of the global PSs, they all fail to find local PSs.

The multimodal multiobjective optimization is a relatively new research direction in the optimization area. Thus, many studies need to be conducted, such as: (1) designing more general MMO test problems, including high-dimensional many-objective MMO test problems with various shapes of PF and PS, (2) developing novel mechanisms to aid the MMO algorithms in finding local and global PSs efficiently, (3) designing algorithms to deal with MMO problems with linkages among variables/objectives, (4) selecting final solutions to MMO problems, (5) visualizing the landscape using high dimensional visualization technology, and (6) visualizing the search process of evolutionary algorithms.

Acknowledgement

We acknowledge financial support by National Natural Science Foundation of China (61473266, 61673404, 61876169, and 61806179), Project supported by the Research Award Fund for Outstanding Young Teachers in Henan Provincial Institutions of Higher Education of China (2014GGJS-004) and Program for Science & Technology Innovation Talents in Universities of Henan Province in China (16HASTIT041 and 16HASTIT033), Scientific and Technological Project of Henan Province (152102210153), China Postdoctoral Science Foundation (2017M622373, 2018M630835).

Appendix A. Supplementary data

Supplementary data to this article can be found online at https://doi.org/10.1016/j.swevo.2019.03.011.

References

[1] M. Preuss, Multimodal Optimization by Means of Evolutionary Algorithms, Springer International Publishing, 2015.
[2] R. Cheng, M. Li, K. Li, X. Yao, Evolutionary multiobjective optimization-based multimodal optimization: fitness landscape approximation and peak detection, IEEE Trans. Evol. Comput. 22 (5) (2018) 692–706.
[3] R. Thomsen, Multimodal optimization using crowding-based differential evolution, in: IEEE Congress on Evolutionary Computation, 2004, pp. 1382–1389.
[4] X. Li, Efficient differential evolution using speciation for multimodal function optimization, in: Conference on Genetic and Evolutionary Computation, 2005, pp. 873–880.
[5] A. Basak, S. Das, K.C. Tan, Multimodal optimization using a biobjective differential evolution algorithm enhanced with mean distance-based selection, IEEE Trans. Evol. Comput. 17 (5) (2013) 666–685.
[6] S. Das, S. Maity, B.Y. Qu, P.N. Suganthan, Real-Parameter evolutionary multimodal optimization — a survey of the state-of-the-art, Swarm Evolut. Comput. 1 (2) (2011) 71–88.
[7] K. Deb, Multi-objective genetic algorithms: problem difficulties and construction of test problems, Evol. Comput. 7 (3) (1999) 205–230.
[8] C. Yue, B. Qu, J.J. Liang, A multiobjective particle swarm optimizer using ring topology for solving multimodal multiobjective problems, IEEE Trans. Evol. Comput. 22 (5) (2018) 805–817.
[9] J.J. Liang, C. Yue, B. Qu, Multimodal multi-objective optimization: a preliminary study, in: IEEE Congress on Evolutionary Computation, 2016, pp. 2454–2461.
[10] P. Kerschke, H. Wang, M. Preuss, C. Grimme, A. Deutz, H. Trautmann, M. Emmerich, Search dynamics on multimodal multi-objective problems, Evol. Comput. (2018), https://doi.org/10.1162/evco_a_00234.
[11] T.T. Nguyen, S. Yang, J. Branke, Evolutionary dynamic optimization: a survey of the state of the art, Swarm Evolut. Comput. 6 (2012) 1–24.
[12] O.M. Shir, M. Preuss, B. Naujoks, M. Emmerich, Enhancing decision space diversity in evolutionary multiobjective algorithms, in: International Conference on Evolutionary Multi-Criterion Optimization, 2009, pp. 95–109.
[13] M. Preuss, C. Kausch, C. Bouvy, F. Henrich, Decision space diversity can Be essential for solving multiobjective real-world problems, in: Multiple Criteria Decision Making for Sustainable Energy and Transportation Systems, vol. 2010, 2010, pp. 367–377.
[14] K. Deb, S. Tiwari, Omni-optimizer: a procedure for single and multi-objective optimization, in: International Conference on Evolutionary Multi-Criterion Optimization, 2005, pp. 47–61.
[15] K. Deb, A. Pratap, S. Agarwal, T. Meyarivan, A fast and elitist multiobjective genetic algorithm: NSGA-II, IEEE Trans. Evol. Comput. 6 (2) (2002) 182–197.
[16] G. Rudolph, B. Naujoks, M. Preuss, Capabilities of EMOA to detect and preserve equivalent Pareto subsets, in: International Conference on Evolutionary Multi-Criterion Optimization, 2007, pp. 36–50.
[17] H. Ishibuchi, Y. Hitotsuyanagi, N. Tsukamoto, Y. Nojima, Many-objective test problems to visually examine the behavior of multiobjective evolution in a decision space, in: International Conference on Parallel Problem Solving from Nature, 2010, pp. 91–100.
[18] H. Ishibuchi, N. Akedo, Y. Nojima, A many-objective test problem for visually examining diversity maintenance behavior in a decision space, in: Conference on Genetic and Evolutionary Computation, 2011, pp. 649–656.
[19] H. Ishibuchi, M. Yamane, N. Akedo, Y. Nojima, Many-objective and many-variable test problems for visual examination of multiobjective search, in: IEEE Congress on Evolutionary Computation, 2013, pp. 1491–1498.
[20] H. Masuda, Y. Nojima, H. Ishibuchi, Visual examination of the behavior of EMO algorithms for many-objective optimization with many decision variables, in: IEEE Congress on Evolutionary Computation, 2014, pp. 2633–2640.
[21] Y. Liu, H. Ishibuchi, Y. Nojima, A double-niched evolutionary algorithm and its behavior on polygon-based problems, in: International Conference on Parallel Problem Solving from Nature, 2018, pp. 262–273.
[22] R. Tanabe, H. Ishibuchi, A decomposition-based evolutionary algorithm for multi-modal multi-objective optimization, in: International Conference on Parallel Problem Solving from Nature, 2018, pp. 249–261.
[23] Y. Liu, G.G. Yen, D. Gong, A multi-modal multi-objective evolutionary algorithm using two-archive and recombination strategies, IEEE Trans. Evol. Comput. (2018), https://doi.org/10.1109/TEVC.2018.2879406. Early Access.
[24] J.J. Liang, Q. Guo, C. Yue, B. Qu, K. Yu, A self-organizing multi-objective particle swarm optimization algorithm for multimodal multi-objective problems, in: International Conference on Swarm Intelligence, 2018, pp. 550–560.
[25] W. Xu, J.J. Liang, C. Yue, B. Qu, Multimodal multi-objective differential evolution algorithm for solving nonlinear equations, Appl. Res. Comput. 35 (6) (2019).
[26] K. Deb, L. Thiele, M. Laumanns, E. Zitzler, Scalable Test Problems for Evolutionary Multiobjective Optimization, Indian Institute of Technology, India, 2001.
[27] P. Kerschke, H. Wang, M. Preuss, C. Grimme, A. Deutz, H. Trautmann, M. Emmerich, Towards analyzing multimodality of multiobjective landscapes, in: International Conference on Parallel Problem Solving from Nature, 2016, pp. 962–972.
[28] B. Qu, J.J. Liang, Z.Y. Wang, Q. Chen, P.N. Suganthan, Novel benchmark functions for continuous multimodal optimization with comparative results, Swarm Evolut. Comput. 26 (2016) 23–34.
[29] X. Li, A. Engelbrecht, M.G. Epitropakis, Benchmark Functions for CEC 2013 Special Session and Competition on Niching Methods for Multimodal Function Optimization, RMIT University, Australia, 2013.
[30] T. Tusar, D. Brockhoff, N. Hansen, A. Auger, COCO: the Bi-objective Black Box Optimization Benchmarking (Bbob-biobj) Test Suite, 2016. arXiv:1604.00359.
[31] A. Ahrari, K. Deb, A novel class of test problems for performance evaluation of niching methods, IEEE Trans. Evol. Comput. (2017), https://doi.org/10.1109/TEVC.2017.2775211. Early Access.
[32] H. Ishibuchi, Y. Setoguchi, H. Masuda, Y. Nojima, Performance of decomposition-based many-objective algorithms strongly depends on Pareto front shapes, IEEE Trans. Evol. Comput. 21 (2) (2017) 169–190.
[33] X. Li, M.G. Epitropakis, K. Deb, A. Engelbrecht, Seeking multiple solutions: an updated survey on niching methods and their applications, IEEE Trans. Evol. Comput. 21 (4) (2017) 518–538.
[34] O. Mersmann, B. Bischl, H. Trautmann, M. Preuss, C. Weihs, G. Rudolph, Exploratory landscape analysis, in: Proceedings of the 13th Annual Conference on Genetic and Evolutionary Computation, 2011, pp. 829–836.
[35] K.M. Malan, A.P. Engelbrecht, A survey of techniques for characterising fitness landscapes and some possible ways forward, Inf. Sci. 241 (2013) 148–163.
[36] C. M. M. d. Fonseca, Multiobjective Genetic Algorithms with Application to Control Engineering Problems, University of Sheffield, 1995.
[37] T. Tušar, B. Filipič, Visualization of Pareto front approximations in evolutionary multiobjective optimization: a critical review and the Prosection method, IEEE Trans. Evol. Comput. 19 (2) (2015) 225–245.
[38] P. Kerschke, C. Grimme, An expedition to multimodal multi-objective optimization landscapes, in: International Conference on Evolutionary Multi-Criterion Optimization, 2017, pp. 329–343.
[39] Q. Zhang, A. Zhou, Y. Jin, Rm-meda: a regularity model-based multiobjective estimation of distribution algorithm, IEEE Trans. Evol. Comput. 12 (1) (2008) 41–63.
[40] A. Zhou, Q. Zhang, Y. Jin, Approximating the set of pareto-optimal solutions in both the decision and objective spaces by an estimation of distribution algorithm, IEEE Trans. Evol. Comput. 13 (5) (2009) 1167–1189.
[41] E. Zitzler, L. Thiele, M. Laumanns, C.M. Fonseca, V.G.D. Fonseca, Performance assessment of multiobjective optimizers: an analysis and review, IEEE Trans. Evol. Comput. 7 (2) (2003) 117–132.

APPENDIX

I. Previous MMO test problems

There are eleven MMO test problems in our previous work. The details of them are listed as follows.

SYM-PART simple

$$\begin{cases} f_1 = (p_1 + a)^2 + {p_2}^2 \\ f_2 = (p_1 - a)^2 + {p_2}^2 \end{cases} \tag{A1}$$

where

$$\begin{cases} p_1 = x_1 - t_1(c + 2a) \\ p_2 = x_2 - t_2 b \end{cases}$$

$$t_i = \mathrm{sgn}(\hat{t}_i) \times \min\left\{|\hat{t}_i|, 1\right\}$$

$$\begin{cases} \hat{t}_1 = \mathrm{sgn}(x_1) \times \left\lceil \dfrac{|x_1| - (a + \frac{c}{2})}{2a + c} \right\rceil \\ \hat{t}_2 = \mathrm{sgn}(x_2) \times \left\lceil \dfrac{|x_2| - \frac{b}{2}}{b} \right\rceil \end{cases}$$

Its search space is

$$x_i \in [-20, 20]\,.$$

Its global PSs are

$$\begin{cases} p_1 \in [-a, a] \\ p_2 = 0 \end{cases}$$

Its global PFs are

$$\begin{cases} f_1 = 4a^2 v^2 \\ f_2 = 4a^2 (1 - v)^2 \end{cases}$$

where $v \in [0,1]$.

SYM-PART rotated

$$\begin{cases} f_1 = (p_1 + a)^2 + {p_2}^2 \\ f_2 = (p_1 - a)^2 + {p_2}^2 \end{cases} \tag{A2}$$

where

$$\begin{cases} p_1 = x_1 - t_1(c + 2a) \\ p_2 = x_2 - t_2 b \end{cases}$$

$$t_i = \mathrm{sgn}(\hat{t}_i) \times \min\left\{|\hat{t}_i|, 1\right\}$$

$$\begin{cases} \hat{t}_1 = \mathrm{sgn}(r_1) \times \left\lceil \dfrac{|r_1| - (a + \frac{c}{2})}{2a + c} \right\rceil \\ \hat{t}_2 = \mathrm{sgn}(r_2) \times \left\lceil \dfrac{|r_2| - \frac{b}{2}}{b} \right\rceil \end{cases}$$

$$\begin{cases} r_1 = (\cos\omega) \times x_1 - (\sin\omega) \times x_2 \\ r_2 = (\sin\omega) \times x_1 + (\cos\omega) \times x_2 \end{cases}$$

Its search space is

$$x_i \in [-20, 20].$$

Its global PSs are

$$\begin{cases} p_1 \in [-a, a] \\ p_2 = 0 \end{cases}$$

Its global PFs are

$$\begin{cases} f_1 = 4a^2 v^2 \\ f_2 = 4a^2 (1-v)^2 \end{cases}$$

where $v \in [0,1]$.

Omni-test

$$\begin{cases} f_1 = \sum_{i=1}^{n} \sin(\pi x_i) \\ f_2 = \sum_{i=1}^{n} \cos(\pi x_i) \end{cases} \tag{A3}$$

Its search space is

$$x_i \in [0, 6].$$

Its global PSs are

$$x_i \in [2m+1, 2m+3/2]$$

where $-n \le f_1 \le 0$.

Its global PFs are

$$f_2 = -\sqrt{n^2 - f_1^2}$$

where $-n \le f_1 \le 0$.

MMF1

$$\begin{cases} f_1 = |x_1 - 2| \\ f_2 = 1 - \sqrt{|x_1 - 2|} + 2(x_2 - \sin(6\pi |x_1 - 2| + \pi))^2 \end{cases} \tag{A4}$$

Its search space is

$$x_1 \in [1, 3],\ x_2 \in [-1, 1].$$

Its global PSs are

$$\begin{cases} x_1 = x_1 \\ x_2 = \sin(6\pi |x_1 - 2| + \pi) \end{cases}$$

where $1 \le x_1 \le 3$.

Its global PFs are

$$f_2 = 1 - \sqrt{f_1}$$

where $0 \le f_1 \le 1$.

MMF2

$$\begin{cases} f_1 = x_1 \\ f_2 = \begin{cases} 1 - \sqrt{x_1} + 2(4(x_2 - \sqrt{x_1})^2 \\ -2\cos(\dfrac{20(x_2 - \sqrt{x_1})\pi}{\sqrt{2}}) + 2), \quad 0 \le x_2 \le 1 \\ \\ 1 - \sqrt{x_1} + 2(4(x_2 - 1 - \sqrt{x_1})^2 \\ -\cos(\dfrac{20(x_2 - 1 - \sqrt{x_1})\pi}{\sqrt{2}}) + 2), 1 < x_2 \le 2 \end{cases} \end{cases} \tag{A5}$$

Its search space is

$$x_1 \in [0, 1],\ x_2 \in [0, 2].$$

Its global PSs are

$$\begin{cases} x_2 = x_2 \\ x_1 = \begin{cases} x_2^2 & 0 \le x_2 \le 1 \\ (x_2 - 1)^2 & 1 < x_2 \le 2 \end{cases} \end{cases}$$

Its global PFs are

$$f_2 = 1 - \sqrt{f_1}$$

where $0 \le f_1 \le 1$.

MMF3

$$\begin{cases} f_1 = x_1 \\ f_2 = \begin{cases} 1 - \sqrt{x_1} + 2(4(x_2 - \sqrt{x_1})^2 - \\ 2\cos(\frac{20(x_2 - \sqrt{x_1})\pi}{\sqrt{2}}) + 2) \\ 0 \le x_2 \le 0.5, 0.5 < x_2 < 1 \& 0.25 < x_1 \le 1 \\ \\ 1 - \sqrt{x_1} + 2(4(x_2 - 0.5 - \sqrt{x_1})^2 \\ -\cos(\frac{20(x_2 - 0.5 - \sqrt{x_1})\pi}{\sqrt{2}}) + 2) \\ 1 \le x_2 \le 1.5, 0 \le x_1 < 0.25 \& 0.5 < x_2 < 1 \end{cases} \end{cases} \quad \text{(A6)}$$

Its search space is

$$x_1 \in [0, 1],\ x_2 \in [0, 1.5].$$

Its global PSs are

$$\begin{cases} x_2 = x_2 \\ x_1 = \begin{cases} x_2^2 & 0 \le x_2 \le 0.5, 0.5 < x_2 < 1 \& 0.25 < x_1 \le 1 \\ (x_2 - 0.5)^2 & 1 \le x_2 \le 1.5, 0 \le x_1 < 0.25 \& 0.5 < x_2 < 1 \end{cases} \end{cases}$$

Its global PFs are

$$f_2 = 1 - \sqrt{f_1}$$

where $0 \le f_1 \le 1$.

MMF4

$$\begin{cases} f_1 = |x_1| \\ f_2 = \begin{cases} 1 - x_1^2 + 2(x_2 - \sin(\pi |x_1|))^2 & 0 \le x_2 < 1 \\ 1 - x_1^2 + 2(x_2 - 1 - \sin(\pi |x_1|))^2 & 1 \le x_2 \le 2 \end{cases} \end{cases} \quad \text{(A7)}$$

Its search space is

$$x_1 \in [-1, 1],\ x_2 \in [0, 2].$$

Its global PSs are

$$\begin{cases} x_1 = x_1 \\ x_2 = \begin{cases} \sin(\pi |x_1|) & 0 \le x_2 \le 1 \\ \sin(\pi |x_1|) + 1 & 1 < x_2 \le 2 \end{cases} \end{cases}$$

Its global PFs are

$$f_2 = 1 - f_1^2$$

where $0 \le f_1 \le 1$.

MMF5

$$\begin{cases} f_1 = |x_1 - 2| \\ f_2 = \begin{cases} 1 - \sqrt{|x_1 - 2|} + 2(x_2 - \sin(6\pi |x_1 - 2| + \pi))^2 & -1 \le x_2 \le 1 \\ 1 - \sqrt{|x_1 - 2|} + 2(x_2 - 2 - \sin(6\pi |x_1 - 2| + \pi))^2 & 1 < x_2 \le 3 \end{cases} \end{cases} \quad \text{(A8)}$$

Its search space is

$$x_1 \in [-1, 3],\ x_2 \in [1, 3].$$

Its global PSs are

$$x_2 = \begin{cases} \sin(6\pi \mid x_1 - 2 \mid +\pi) & -1 \le x_2 \le 1 \\ \sin(6\pi \mid x_1 - 2 \mid +\pi) + 2 & 1 < x_2 \le 3 \end{cases}$$

Its global PFs are

$$f_2 = 1 - \sqrt{f_1}$$

where $0 \le f_1 \le 1$.

MMF6

$$\begin{cases} f_1 = |x_1 - 2| \\ f_2 = \begin{cases} 1 - \sqrt{|x_1 - 2|} + 2(x_2 - \sin(6\pi |x_1 - 2| + \pi))^2 & -1 \le x_2 \le 1 \\ 1 - \sqrt{|x_1 - 2|} + 2(x_2 - 1 - \sin(6\pi |x_1 - 2| + \pi))^2 & 1 < x_2 \le 3 \end{cases} \end{cases} \quad \text{(A9)}$$

Its search space is

$$x_1 \in [-1, 3],\ x_2 \in [1, 2].$$

Its global PSs are

$$x_2 = \begin{cases} \sin(6\pi \mid x_1 - 2 \mid +\pi) & -1 \le x_2 \le 1 \\ \sin(6\pi \mid x_1 - 2 \mid +\pi) + 1 & 1 < x_2 \le 2 \end{cases}$$

Its global PFs are

$$f_2 = 1 - \sqrt{f_1}$$

where $0 \le f_1 \le 1$.

MMF7

$$\begin{cases} f_1 = |x_1 - 2| \\ f_2 = 1 - \sqrt{|x_1 - 2|} + \{x_2 - [0.3|x_1 - 2|^2 \cdot \cos(24\pi |x_1 - 2| \\ \qquad +4\pi) + 0.6|x_1 - 2|] \cdot \sin(6\pi |x_1 - 2| + \pi)\}^2 \end{cases} \quad \text{(A10)}$$

Its search space is

$$x_1 \in [1, 3],\ x_2 \in [-1, 1].$$

Its global PSs are

$$x_2 = [0.3|x_1 - 2|^2 \cos(24\pi |x_1 - 2| + 4\pi) + 0.6|x_1 - 2|] \cdot \sin(6\pi |x_1 - 2| + \pi)$$

where $1 \le x_1 \le 3$.

Its global PFs are

$$f_2 = 1 - \sqrt{f_1}$$

where $0 \le f_1 \le 1$.

MMF8

$$\begin{cases} f_1 = \sin|x_1| \\ f_2 = \begin{cases} \sqrt{1 - (\sin|x_1|)^2} + 2(x_2 - \sin|x_1| - |x_1|)^2 & 0 \le x_2 \le 4 \\ \sqrt{1 - (\sin|x_1|)^2} + 2(x_2 - 4 - \sin|x_1| - |x_1|)^2 & 4 < x_2 \le 9 \end{cases} \end{cases} \quad \text{(A11)}$$

Its search space is

$$x_1 \in [-\pi, \pi],\ x_2 \in [0, 9].$$

Its global PSs are

$$x_2 = \begin{cases} \sin|x_1| + |x_1| & 0 \le x_2 \le 4 \\ \sin|x_1| + |x_1| + 4 & 4 < x_2 \le 9 \end{cases}$$

where $-\pi \le x_1 \le \pi$.

Its global PFs are

$$f_2 = 1 - \sqrt{f_1}$$

where $0 \le f_1 \le 1$.

II. Novel MMO test problems

MMF1_z

$$\text{Min} \begin{cases} f_1 = |x_1 - 2| \\ f_2 = \begin{cases} 1 - \sqrt{|x_1 - 2|} + 2(x_2 - \sin(2k\pi|x_1 - 2| + \pi))^2, & x_1 \in [1, 2) \\ 1 - \sqrt{|x_1 - 2|} + 2(x_2 - \sin(2\pi|x_1 - 2| + \pi))^2, & x_1 \in [2, 3] \end{cases} \end{cases} \tag{A12}$$

where $k > 0$ (k controls the deformation degree of the global PS in $x_1 \in [1, 2)$).

Its search space is

$$x_1 \in [1, 3], x_2 \in [-1, 1].$$

Its global PSs are

$$x_2 = \begin{cases} \sin(2k\pi|x_1 - 2| + \pi), & x_1 \in [1, 2) \\ \sin(2\pi|x_1 - 2| + \pi), & x_1 \in [2, 3] \end{cases}$$

where $k > 0$.

Its global PF is

$$f_2 = 1 - \sqrt{f_1}, \ f_1 \in [0, 1] \tag{A13}$$

When $k = 3$, its true PSs and PF are shown in Fig. A1.

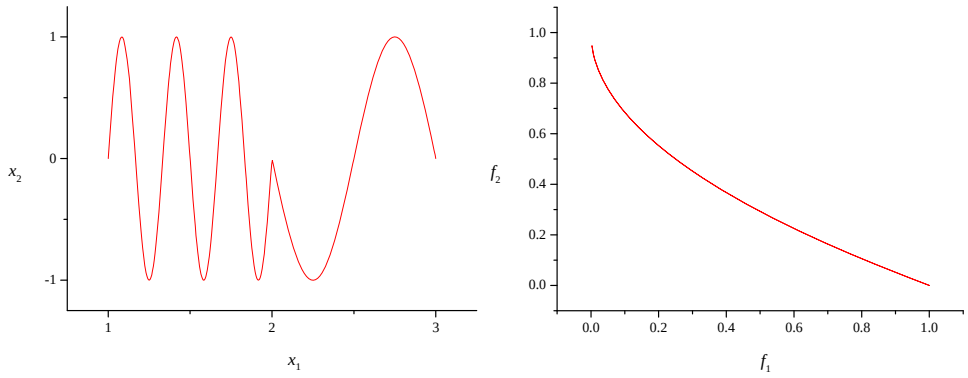

(a) True PSs of MMF1_z (b)True PFs of MMF1_z

Fig. A1. The true PSs and PF of MMF1_z.

MMF1_e

$$\text{Min} \begin{cases} f_1 = |x_1 - 2| \\ f_2 = \begin{cases} 1 - \sqrt{|x_1 - 2|} + 2(x_2 - \sin(6\pi|x_1 - 2| + \pi))^2, & x_1 \in [1, 2) \\ 1 - \sqrt{|x_1 - 2|} + 2(x_2 - a^{x_1}\sin(6\pi|x_1 - 2| + \pi))^2, & x_1 \in [2, 3] \end{cases} \end{cases} \tag{A14}$$

where $a > 0 \,\&\, a \ne 1$ (a controls the amplitude of the global PS in $x_1 \in [2, 3]$).

Its search space is

$$x_1 \in [1, 3], x_2 \in [-a^3, a^3].$$

Its global PSs are

$$x_2 = \begin{cases} \sin(6\pi|x_1 - 2| + \pi), & x_1 \in [1, 2) \\ a^{x_1}\sin(2\pi|x_1 - 2| + \pi), & x_1 \in [2, 3] \end{cases}$$

where $a > 0 \,\&\, a \ne 1$.

Its global PF is

$$f_2 = 1 - \sqrt{f_1}, \ f_1 \in [0, 1] \tag{A15}$$

When $a = e$, its true PSs and PF are shown in Fig. A2.

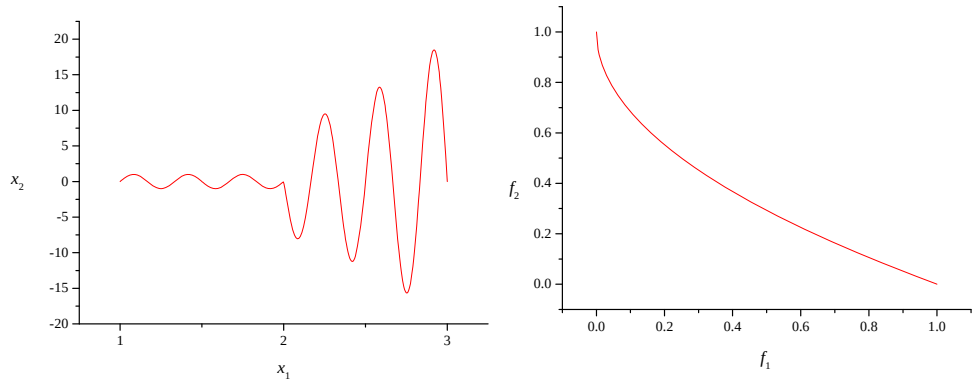

(a) True PSs of MMF1_e (b)True PFs of MMF1_e

Fig. A2. The true PSs and PF of MMF1_e.

MMF9

$$\text{Min} \begin{cases} f_1 = x_1 \\ f_2 = \dfrac{g(x_2)}{x_1} \end{cases} \tag{A16}$$

where $g(x) = 2 - \sin^6\left(n_p \pi x\right)$, n_p is the number of global PSs.

Its search space is

$$x_1 \in [0.1, 1.1], \; x_2 \in [0.1, 1.1].$$

Its i^{th} global PS is

$$x_2 = \frac{1}{2n_p} + \frac{1}{n_p} \cdot (i-1), \; x_1 \in [0.1, 1.1]$$

where $i = 1, 2, \ldots, n_p$.

Its ~~i^{th}~~ global PF is

$$f_2 = \frac{g\left(\dfrac{1}{2n_p}\right)}{f_1}, \; f_1 \in [0.1, 1.1]$$

When $n_p = 2$, its true PSs and PF are shown in Fig. A3.

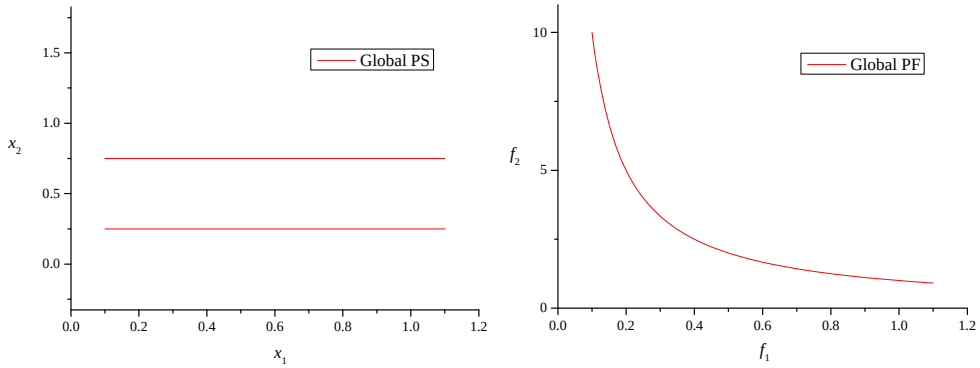

(a) True PSs of MMF9 (b)True PFs of MMF9

Fig. A3. The true PSs and PFs of MMF9.

MMF9_r

$$\text{Min} \begin{cases} f_1 = x_{r1} + A \\ f_2 = \dfrac{g(x_{r2})}{x_{r1}} + A \end{cases} \tag{A17}$$

where $g(x_{r2}) = 2 - \sin^6\left(n_p \pi x_{r2}\right)$, n_p is the number of global PSs. $x_r = xM$, where M is a rotation matrix. $A = \sum_{i=1}^{n} \left(x_{ri} < x_{li}\right) \cdot 10 \cdot \left(1 + \left(x_{ri} - x_{li}\right)^2\right) + \sum_{i=1}^{n} \left(x_{ri} > x_{li}\right) \cdot 10 \cdot \left(1 + \left(x_{ri} - x_{ui}\right)^2\right)$ where n is the number of variables, x_l is the low bound

of x and x_u is the up bound. The A is an additional items to worsen the function values of points outside the original bound after rotation.

Its search space is

$$x \in [-0.5, 0.5].$$

Its i^{th} global PS is

$$x_2 = x_1 + \sqrt{2}\left(\frac{1}{2n_p} + \frac{1}{n_p}\cdot(i-1) - 0.5\right)$$

where $i = 1, 2, \ldots, n_p$.

Its global PF is calculated by its PS and objective functions.

When $n_p = 2$, its true PSs and PF are shown in Fig. A4.

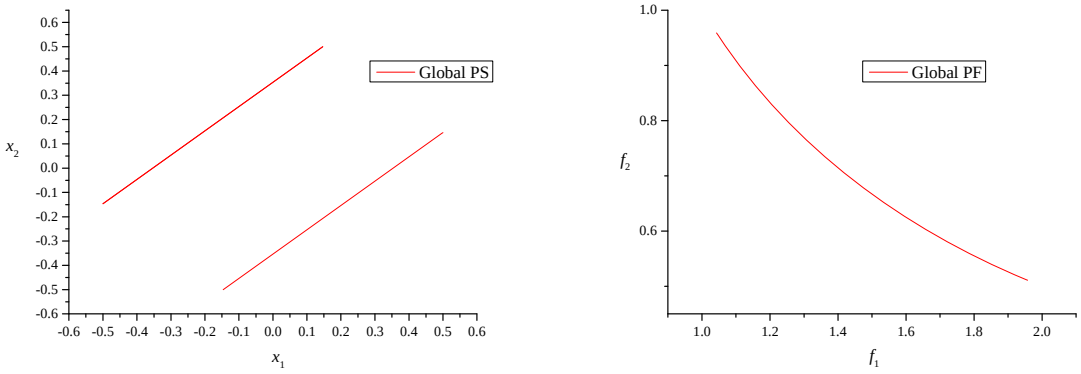

(a) True PSs of MMF9_r (b)True PFs of MMF9_r

Fig. A4. The true PSs and PFs of MMF9_r.

MMF10

$$\text{Min} \begin{cases} f_1 = x_1 \\ f_2 = \dfrac{g(x_2)}{x_1} \end{cases} \tag{A18}$$

where $g(x) = 2 - \exp\left[-\left(\frac{x-0.2}{0.004}\right)^2\right] - 0.8\exp\left[-\left(\frac{x-0.6}{0.4}\right)^2\right]$.

Its search space is

$$x_1 \in [0.1, 1.1],\ x_2 \in [0.1, 1.1].$$

Its global PS is

$$x_2 = 0.2,\ x_1 \in [0.1, 1.1].$$

Its local PS is

$$x_2 = 0.6,\ x_1 \in [0.1, 1.1].$$

Its global PF is

$$f_2 = \frac{g(0.2)}{f1},\ f_1 \in [0.1, 1.1].$$

Its local PF is

$$f_2 = \frac{g(0.6)}{f1},\ f_1 \in [0.1, 1.1].$$

Its true PSs and PFs are shown in Fig. A5.

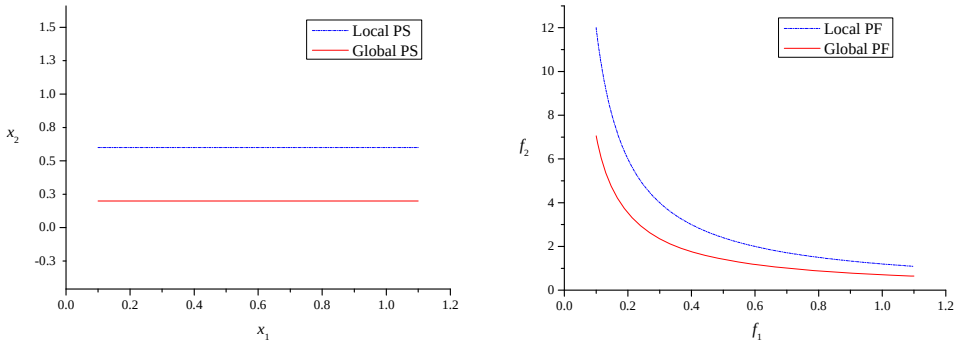

(a) True PSs of MMF10 (b) True PFs of MMF10

Fig. A5. The true PSs and PFs of MMF10.

MMF11

$$\text{Min} \begin{cases} f_1 = x_1 \\ f_2 = \dfrac{g(x_2)}{x_1} \end{cases} \tag{A19}$$

where $g(x) = 2 - \exp\left[-2\log(2)\cdot\left(\dfrac{x-0.1}{0.8}\right)^2\right]\cdot\sin^6\left(n_p\pi x\right)$, n_p is the total number of global and local PSs.

Its search space is

$$x_1 \in [0.1, 1.1],\ x_2 \in [0.1, 1.1].$$

Its global PS is

$$x_2 = \frac{1}{2n_p},\ x_1 \in [0.1, 1.1].$$

Its i^{th} local PS is

$$x_2 = \frac{1}{2n_p} + \frac{1}{n_p}\cdot(i-1),\ x_1 \in [0.1, 1.1]$$

where $i = 2, 3, \ldots, n_p$.

Its global PF is

$$f_2 = \frac{g\left(\dfrac{1}{2n_p}\right)}{f_1},\ f_1 \in [0.1, 1.1].$$

Its local PF is

$$f_2 = \frac{g\left(\dfrac{1}{2n_p} + \dfrac{1}{n_p}\cdot(i-1)\right)}{f_1},\ f_1 \in [0.1, 1.1]$$

where $i = 2, 3, \ldots, n_p$.

When $n_p = 2$, its true PSs and PFs are shown in Fig. A6.

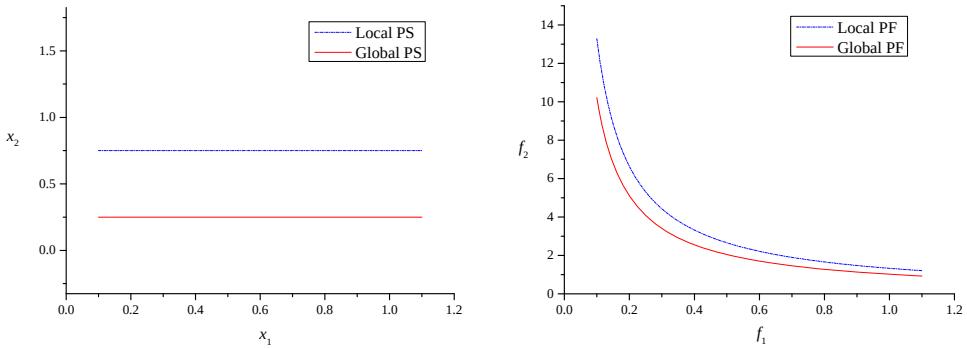

(a) True PSs of MMF11 (b) True PFs of MMF11

Fig. A6. The true PSs and PFs of MMF11.

MMF12

$$\text{Min} \begin{cases} f_1 = x_1 \\ f_2 = g(x_2) \cdot h(f_1, g) \end{cases} \tag{A20}$$

where $g(x) = 2 - \exp\left[-2\log(2) \cdot \left(\frac{x-0.1}{0.8}\right)^2\right] \cdot \sin^6\left(n_p \pi x\right)$, n_p is the total number of global and local PSs,

$h(f_1, g) = 1 - \left(\frac{f_1}{g}\right)^2 - \frac{f_1}{g}\sin(2\pi q f_1)$, q is the number of discontinuous pieces in each PF (PS).

Its search space is

$$x_1 \in [0,1],\ x_2 \in [0,1].$$

Its global PS is discontinuous pieces in

$$x_2 = \frac{1}{2n_p}.$$

Its i^{th} local PSs are discontinuous pieces in

$$x_2 = \frac{1}{2n_p} + \frac{1}{n_p} \cdot (i-1)$$

where $i = 2, 3, \ldots, n_p$.

Its global PF is discontinuous pieces in

$$f_2 = g^* \cdot h(f_1, g^*)$$

where g^* is the global optimum of $g(x)$.

Its local PFs are discontinuous pieces in

$$f_2 = g_l^* \cdot h(f_1, g_l^*)$$

where g_l^* are the local optima of $g(x)$.

The ranges of discontinuous pieces depend on the minima of $f_2 = g^* \cdot h(f_1, g^*)$.

When $n_p = 2$, its true PSs and PFs are shown in Fig. A7.

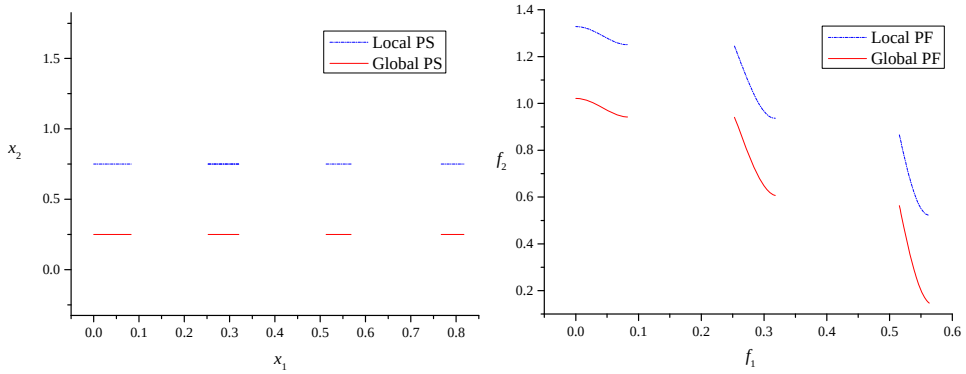

(a) True PSs of MMF12 (b) True PFs of MMF12

Fig. A7. The true PSs and PFs of MMF12.

MMF13

$$\min \begin{cases} f_1 = x_1 \\ f_2 = \dfrac{g(t)}{x_1} \end{cases} \tag{A21}$$

where $g(t) = 2 - \exp\left[-2\log(2) \cdot \left(\frac{t-0.1}{0.8}\right)^2\right] \cdot \sin^6\left(n_p \pi(t)\right)$,

$t = x_2 + \sqrt{x_3}$, n_p is the total number of global and local PSs.

Its search space is

$$x_1 \in [0.1,1.1],\ x_2 \in [0.1,1.1],\ x_3 \in [0.1,1.1].$$

Its global PS is

$$x_2+\sqrt{x_3}=\frac{1}{2n_p},\ x_1\in[0.1,1.1].$$

Its i^{th} local PSs is

$$x_2+\sqrt{x_3}=\frac{1}{2n_p}+\frac{i-1}{n_p},\ x_1\in[0.1,1.1].$$

where $i=2,3,\ldots,n_p$.

Its global PF is

$$f_2=\frac{2-\exp\left[-2\log(2)\cdot\left(\frac{\frac{1}{2n_p}-0.1}{0.8}\right)^2\right]\cdot\sin^6\left(n_p\pi\left(\frac{1}{2n_p}\right)\right)}{f_1}$$

Its local PFs are

$$f_2=\frac{2-\exp\left[-2\log(2)\cdot\left(\frac{\left(\frac{1}{2n_p}+\frac{i-1}{n_p}\right)-0.1}{0.8}\right)^2\right]\cdot\sin^6\left(n_p\pi\left(\frac{1}{2n_p}+\frac{i-1}{n_p}\right)\right)}{f_1}$$

where $i=2,3,\ldots,n_p$.

When $n_p=2$, its true PSs and PFs are shown in Fig. A8.

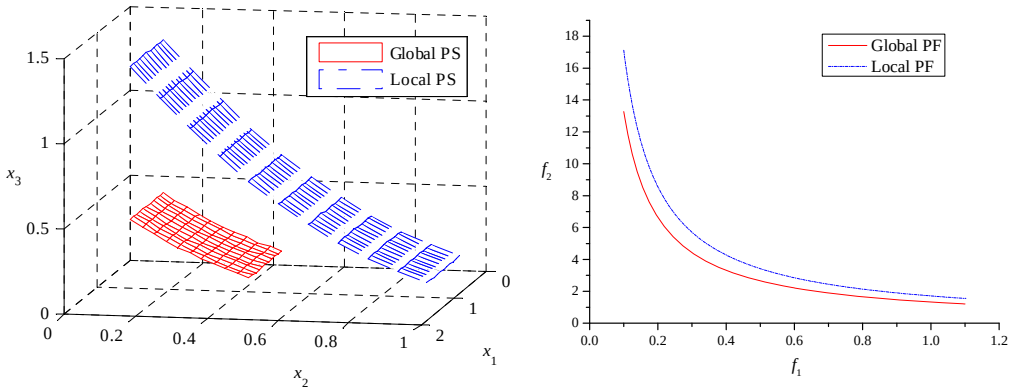

(a) True PSs of MMF13 (b) True PFs of MMF13

Fig. A8. The true PSs and PFs of MMF13.

MMF14

$$\text{Min}\begin{cases} f_1=\cos(\pi/2\,x_1)\cos(\pi/2\,x_2)\cdots\cos(\pi/2\,x_{m-2})\cos(\pi/2\,x_{m-1})\left(1+g(x_m,x_{m+1},\ldots,x_{m-1+k})\right)\\ f_2=\cos(\pi/2\,x_1)\cos(\pi/2\,x_2)\cdots\cos(\pi/2\,x_{m-2})\sin(\pi/2\,x_{m-1})\left(1+g(x_m,x_{m+1},\ldots,x_{m-1+k})\right)\\ f_3=\cos(\pi/2\,x_1)\cos(\pi/2\,x_2)\cdots\sin(\pi/2\,x_{m-2})\left(1+g(x_m,x_{m+1},\ldots,x_{m-1+k})\right)\\ \vdots\\ f_{m-1}=\cos(\pi/2\,x_1)\sin(\pi/2\,x_2)\left(1+g(x_m,x_{m+1},\ldots,x_{m-1+k})\right)\\ f_m=\sin(\pi/2\,x_1)\left(1+g(x_m,x_{m+1},\ldots,x_{m-1+k})\right)\end{cases} \tag{A22}$$

where $g(x_m,x_{m+1},\ldots,x_{m-1+k})=2-\sin^2\left(n_p\pi\left(x_{m-1+k}\right)\right)$, n_p is the number of global PSs.

Its search space is

$$x_i\in[0,1],\text{ for } i=1,2,\ldots,n,$$

where n is the dimension of decision space; m is the dimension of objective space; $k=n-(m-1)$.

Its i^{th} (i = 1, 2,…, n_p) global PSs are

$$x_n = \frac{1}{2n_p} + \frac{1}{n_p}\cdot(i-1),\ x_j \in [0,1] \text{ for } j = 1:n-1.$$

Its global PFs are

$$\sum_{j=1}^{M}\left(f_j\right)^2 = (1+g^*)^2$$

where g^* are the global optima of $g(x)$.

When $n_p = 2, m = 2, n = 3$, its true PSs and PFs are shown in Fig. A9.

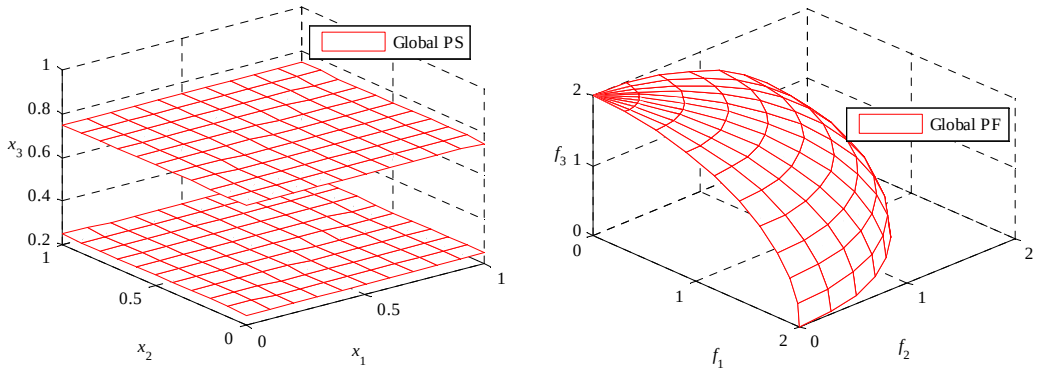

(a) True PSs of MMF14 (b) True PFs of MMF14

Fig. A9. The true PSs and PFs of MMF14.

MMF14_a

$$\text{Min}\begin{cases} f_1 = \cos(\pi/2\, x_1)\cos(\pi/2\, x_2)\cdots\cos(\pi/2\, x_{m-2})\cos(\pi/2\, x_{m-1})\left(1+g(x_m, x_{m+1},\ldots, x_{m-1+k})\right) \\ f_2 = \cos(\pi/2\, x_1)\cos(\pi/2\, x_2)\cdots\cos(\pi/2\, x_{m-2})\sin(\pi/2\, x_{m-1})\left(1+g(x_m, x_{m+1},\ldots, x_{m-1+k})\right) \\ f_3 = \cos(\pi/2\, x_1)\cos(\pi/2\, x_2)\cdots\sin(\pi/2\, x_{m-2})\left(1+g(x_m, x_{m+1},\ldots, x_{m-1+k})\right) \\ \vdots \\ f_{m-1} = \cos(\pi/2\, x_1)\sin(\pi/2\, x_2)\left(1+g(x_m, x_{m+1},\ldots, x_{m-1+k})\right) \\ f_m = \sin(\pi/2\, x_1)\left(1+g(x_m, x_{m+1},\ldots, x_{m-1+k})\right) \end{cases} \quad \text{(A23)}$$

where $g(x_m, x_{m+1},\ldots, x_{m-1+k}) = 2-\sin^2\left(n_p\pi\left(x_{m-1+k} - 0.5\sin\left(\pi x_{m-2+k}\right) + \frac{1}{2n_p}\right)\right)$, n_p is the number of global PSs.

Its search space is

$$x_i \in [0, 1], \text{ for } i = 1, 2,\ldots, n$$

where n is the dimension of decision space; m is the dimension of objective space; $k = n-(m-1)$.

Its i^{th} (i = 1, 2,…, n_p) global PSs are

$$x_n = 0.5\sin\left(\pi x_{n-1}\right) + \frac{1}{n_p}\cdot(i-1),\ x_j \in [0,1] \text{ for } j = 1:n-1.$$

Its global PFs are

$$\sum_{j=1}^{M}\left(f_j\right)^2 = (1+g^*)^2$$

where g^* are the global optima of $g(x)$.

When $n_p = 2, m = 2, n = 3$, its true PSs and PFs are shown in Fig. A10.

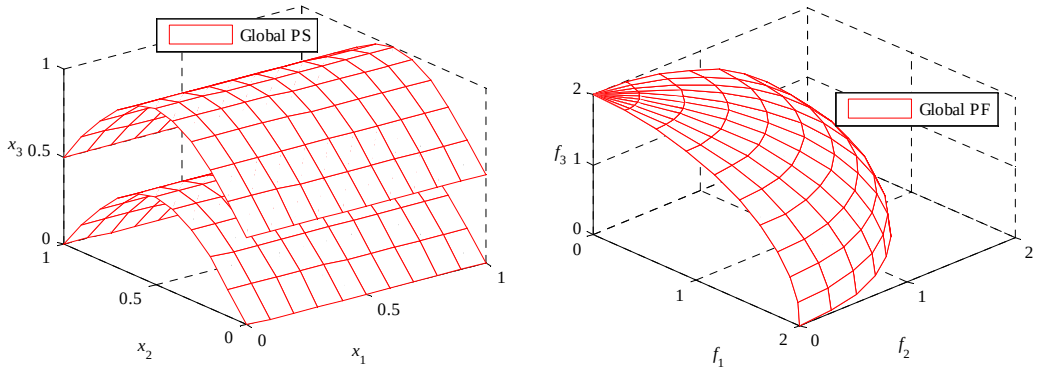

(a) True PSs of MMF14_a (b) True PFs of MMF14_a

Fig. A10. The true PSs and PFs of MMF14_a.

MMF15

$$\text{Min}\begin{cases} f_1 = \cos(\pi/2\, x_1)\cos(\pi/2\, x_2)\cdots\cos(\pi/2\, x_{m-2})\cos(\pi/2\, x_{m-1})\left(1+g(x_m, x_{m+1},\ldots, x_{m-1+k})\right) \\ f_2 = \cos(\pi/2\, x_1)\cos(\pi/2\, x_2)\cdots\cos(\pi/2\, x_{m-2})\sin(\pi/2\, x_{m-1})\left(1+g(x_m, x_{m+1},\ldots, x_{m-1+k})\right) \\ f_3 = \cos(\pi/2\, x_1)\cos(\pi/2\, x_2)\cdots\sin(\pi/2\, x_{m-2})\left(1+g(x_m, x_{m+1},\ldots, x_{m-1+k})\right) \\ \vdots \\ f_{m-1} = \cos(\pi/2\, x_1)\sin(\pi/2\, x_2)\left(1+g(x_m, x_{m+1},\ldots, x_{m-1+k})\right) \\ f_m = \sin(\pi/2\, x_1)\left(1+g(x_m, x_{m+1},\ldots, x_{m-1+k})\right) \end{cases} \tag{A24}$$

where $g(x_m, x_{m+1},\ldots, x_{m-1+k}) = 2-\exp\left[-2\log(2)\cdot\left(\frac{x_{m-1+k}-0.1}{0.8}\right)^2\right]\cdot\sin^2\left(n_p\pi x_{m-1+k}\right)$, n_p is the number of global PSs.

Its search space is

$$x_i \in [0,1], \text{ for } i = 1, 2,\ldots, n,$$

where n is the dimension of decision space; m is the dimension of objective space; $k = n-(m-1)$.

Its global PS is

$$x_n = \frac{1}{2n_p},\ x_j \in [0,1] \text{ for } j = 1:n-1.$$

Its i^{th} (i = 2, 3,…, n_p) local PSs are

$$x_n = \frac{1}{2n_p}+\frac{1}{n_p}\cdot(i-1),\ x_j \in [0,1] \text{ for } j = 1:n-1.$$

Its global PF is

$$\sum_{j=1}^{M}\left(f_j\right)^2 = (1+g^*)^2$$

where g^* is the global optimum of $g(x)$.

Its i^{th} local PFs are

$$\sum_{j=1}^{M}\left(f_j\right)^2 = (1+g_l^*)^2$$

where g_l^* are the local optima of $g(x)$.

When $n_p = 2, m = 2, n = 3$, its true PSs and PFs are shown in Fig. A11.

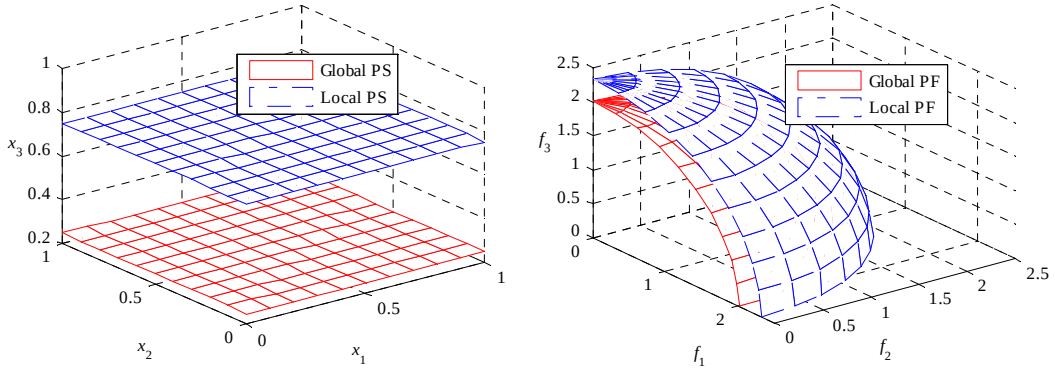

(a) True PSs of MMF15 (b) True PFs of MMF15

Fig. A11. The true PSs and PFs of MMF15.

MMF15_a

$$\text{Min}\begin{cases} f_1 = \cos(\pi/2\, x_1)\cos(\pi/2\, x_2)\cdots\cos(\pi/2\, x_{m-2})\cos(\pi/2\, x_{m-1})\left(1+g(x_m, x_{m+1},\ldots, x_{m-1+k})\right) \\ f_2 = \cos(\pi/2\, x_1)\cos(\pi/2\, x_2)\cdots\cos(\pi/2\, x_{m-2})\sin(\pi/2\, x_{m-1})\left(1+g(x_m, x_{m+1},\ldots, x_{m-1+k})\right) \\ f_3 = \cos(\pi/2\, x_1)\cos(\pi/2\, x_2)\cdots\sin(\pi/2\, x_{m-2})\left(1+g(x_m, x_{m+1},\ldots, x_{m-1+k})\right) \\ \vdots \\ f_{m-1} = \cos(\pi/2\, x_1)\sin(\pi/2\, x_2)\left(1+g(x_m, x_{m+1},\ldots, x_{m-1+k})\right) \\ f_m = \sin(\pi/2\, x_1)\left(1+g(x_m, x_{m+1},\ldots, x_{m-1+k})\right) \end{cases} \quad \text{(A25)}$$

where $g(x_m, x_{m+1},\ldots, x_{m-1+k}) = 2-\exp\left[-2\log(2)\cdot\left(\frac{t-0.1}{0.8}\right)^2\right]\cdot\sin^2\left(n_p\pi t\right)$, $t = x_{m-1+k} - 0.5\sin\left(\pi x_{m-2+k}\right)+\frac{1}{2n_p}$, n_p is the number of global PSs.

Its search space is

$$x_i \in [0,1], \text{ for } i = 1, 2,\ldots, n$$

where n is the dimension of decision space; m is the dimension of objective space; $k = n-(m-1)$.

Its global PS is

$$x_n = 0.5\sin\left(\pi x_{n-1}\right),\ x_j \in [0,1] \text{ for } j = 1:n-1.$$

Its i^{th} (i = 2, 3,…, n_p) local PSs are

$$x_n = 0.5\sin\left(\pi x_{n-1}\right)+\frac{1}{n_p}(i-1),\ x_j \in [0,1] \text{ for } j = 1:n-1.$$

Its global PF is

$$\sum_{j=1}^{M}\left(f_j\right)^2 = (1+g^*)^2$$

where g^* is the global optimum of $g(x)$.

Its i^{th} local PFs are

$$\sum_{j=1}^{M}\left(f_j\right)^2 = (1+g_l^*)^2$$

where g_l^* are the local optima of $g(x)$.

When $n_p = 2, m = 2, n = 3$, its true PSs and PFs are shown in Fig. A12.

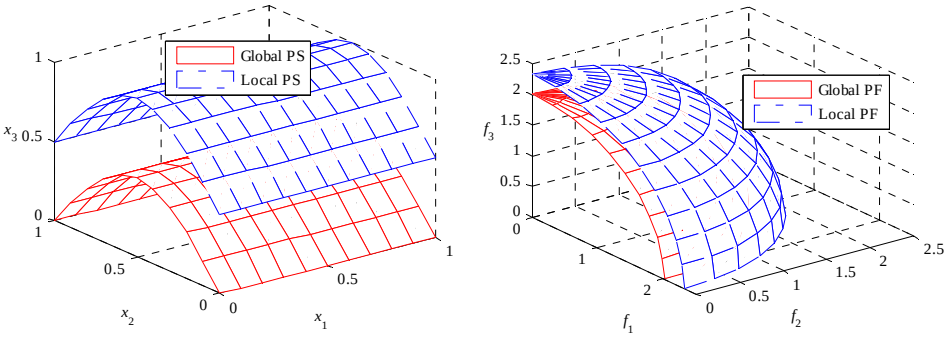

(a) True PSs of MMF15_a (b) True PFs of MMF15_a

Fig. A12. The true PSs and PFs of MMF15_a.

III. The PSs obtained by different algorithms

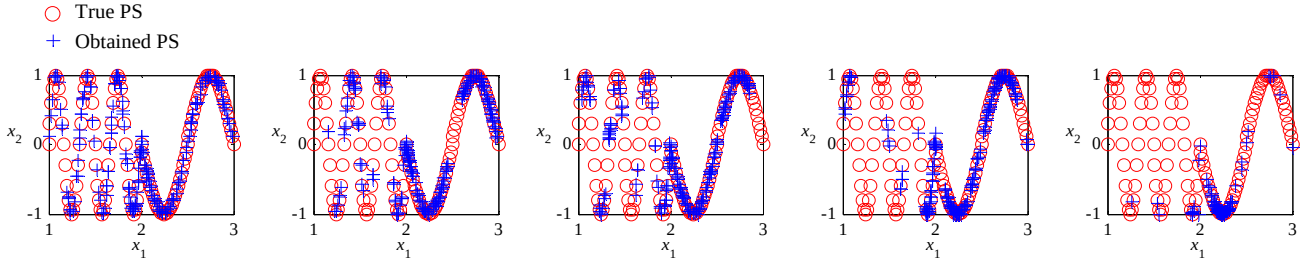

(a) MO_Ring_PSO_SCD (b) DN-NSGAII (c) Omni-optimizer (d) NSGAII (e) SPEA2

Fig. A13. The comparison of PSs obtained by different algorithms on MMF1_z.

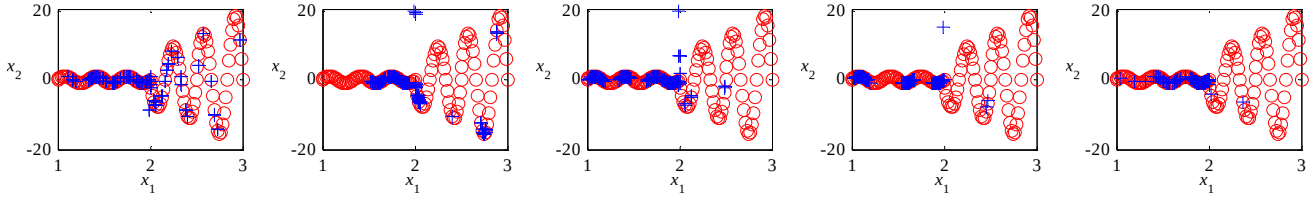

(a) MO_Ring_PSO_SCD (b) DN-NSGAII (c) Omni-optimizer (d) NSGAII (e) SPEA2

Fig. A14. The comparison of PSs obtained by different algorithms on MMF1_e.

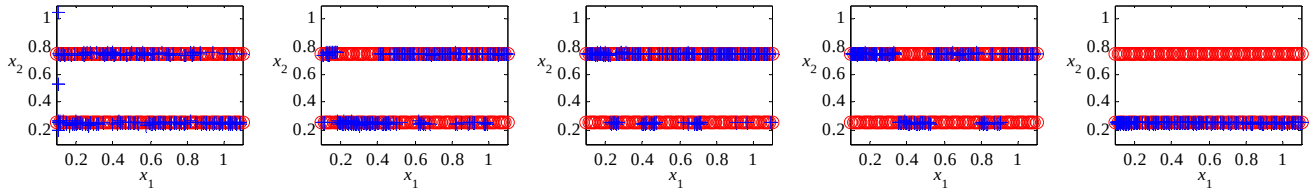

(a) MO_Ring_PSO_SCD (b) DN-NSGAII (c) Omni-optimizer (d) NSGAII (e) SPEA2

Fig. A15. The comparison of PSs obtained by different algorithms on MMF9.

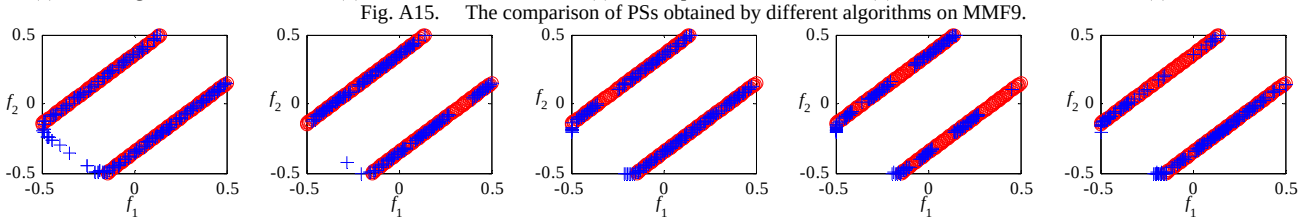

(a) MO_Ring_PSO_SCD (b) DN-NSGAII (c) Omni-optimizer (d) NSGAII (e) SPEA2

Fig. A16. The comparison of PSs obtained by different algorithms on MMF9_r.

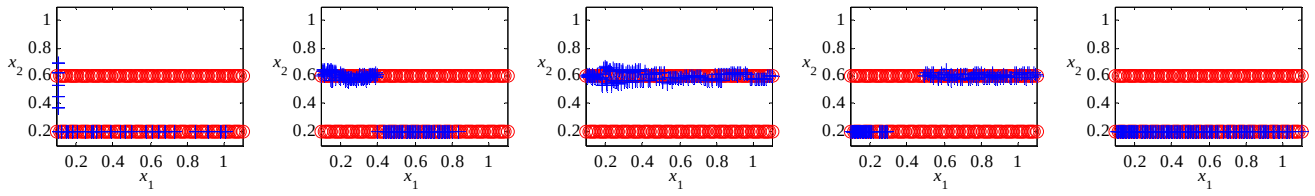

(a) MO_Ring_PSO_SCD (b) DN-NSGAII (c) Omni-optimizer (d) NSGAII (e) SPEA2

Fig. A17. The comparison of PSs obtained by different algorithms on MMF10.

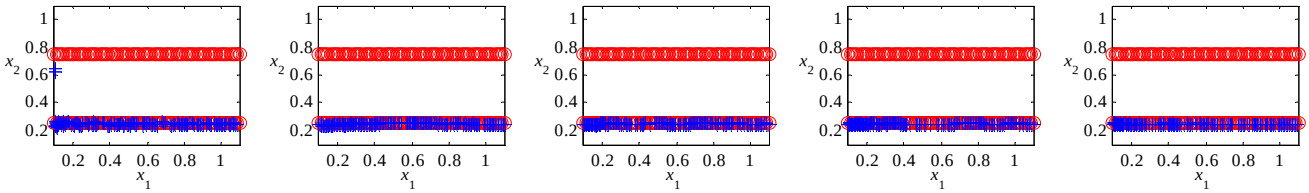

(a) MO_Ring_PSO_SCD (b) DN-NSGAII (c) Omni-optimizer (d) NSGAII (e) SPEA2

Fig. A18. The comparison of PSs obtained by different algorithms on MMF11.

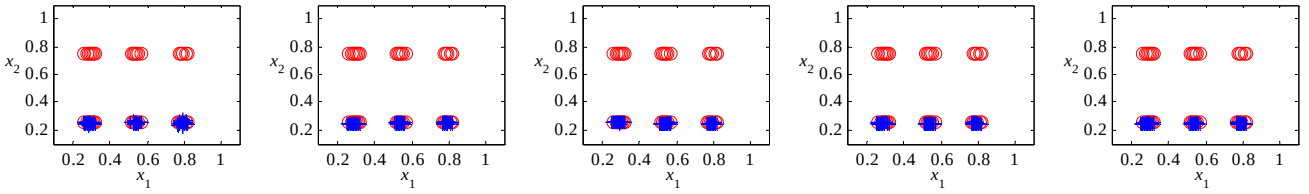

(a) MO_Ring_PSO_SCD (b) DN-NSGAII (c) Omni-optimizer (d) NSGAII (e) SPEA2

Fig. A19. The comparison of PSs obtained by different algorithms on MMF12.

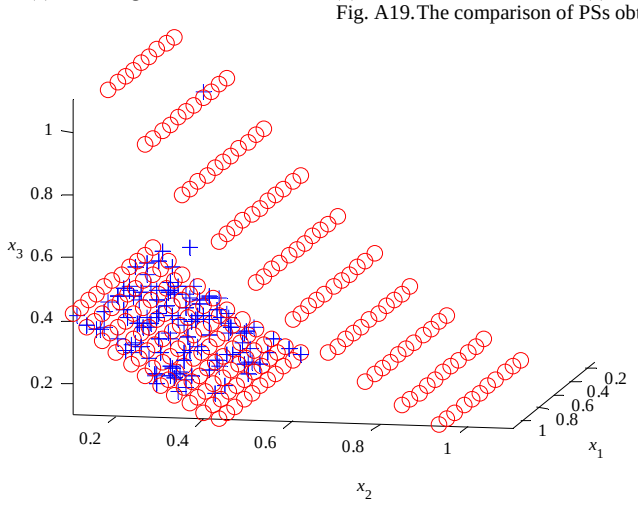

(a) MO_Ring_PSO_SCD

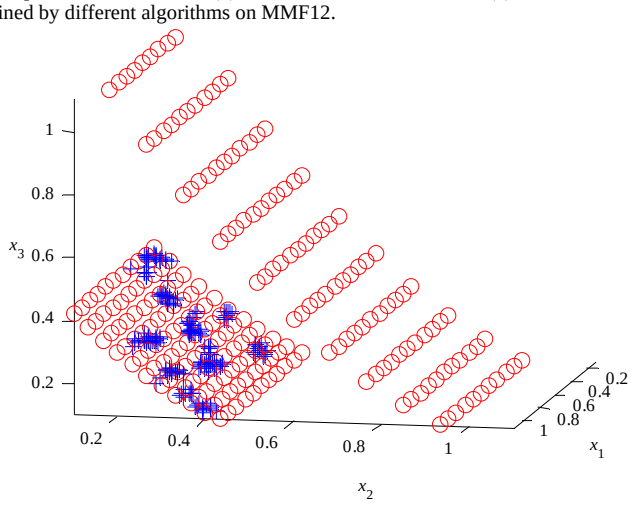

(b) DN-NSGAII

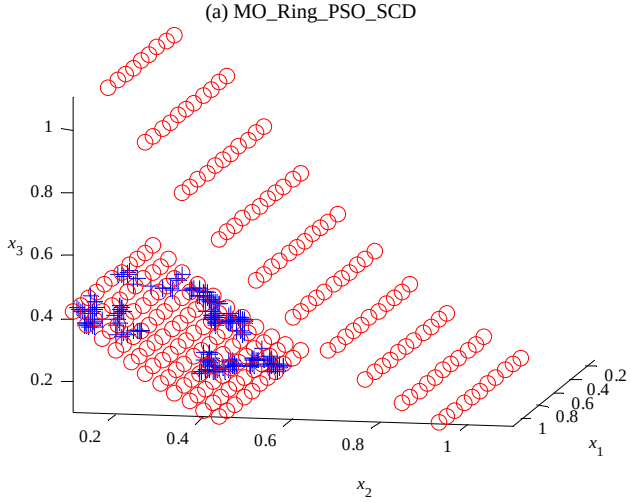

(c) Omni-optimizer

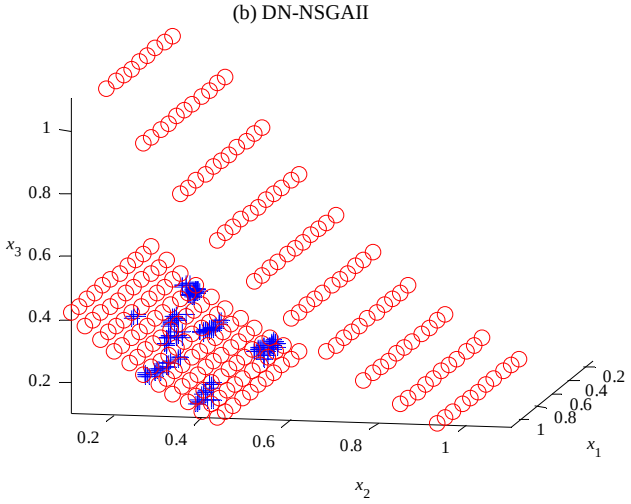

(d) NSGAII

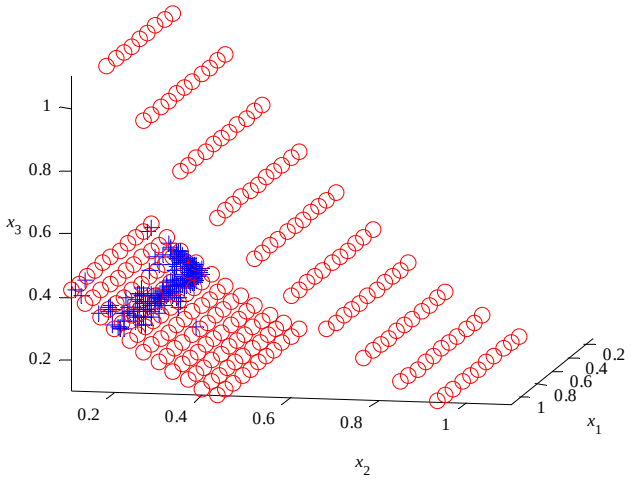

(e) SPEA2

Fig. A20. The comparison of PSs obtained by different algorithms on MMF13.

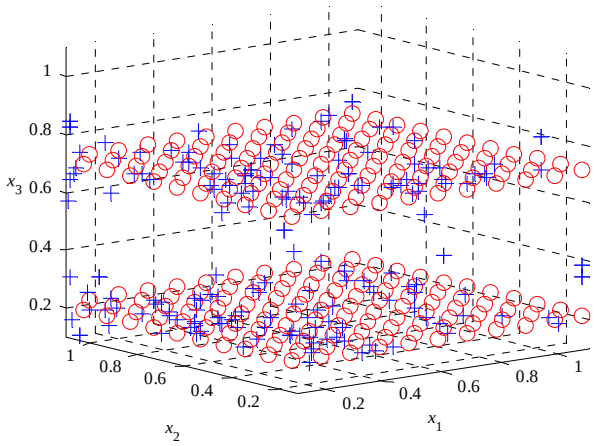

(a) MO_Ring_PSO_SCD

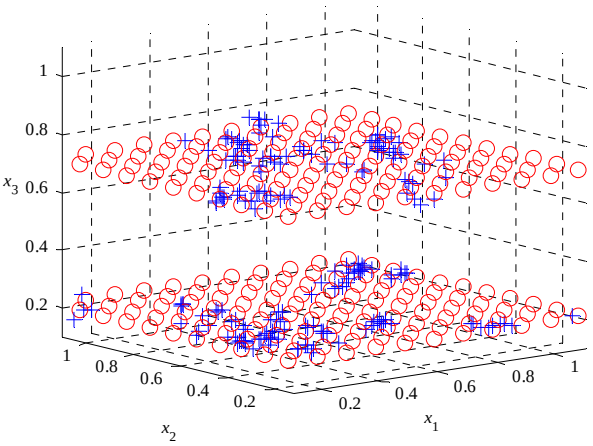

(b) DN-NSGAII

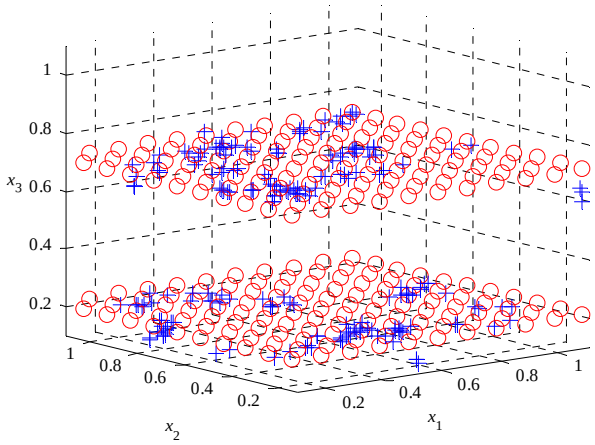

(c) Omni-optimizer

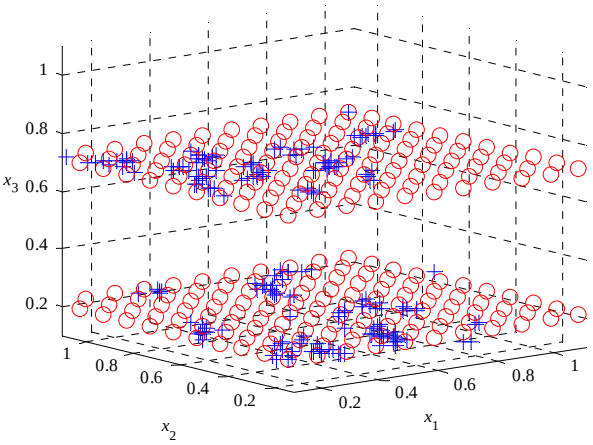

(d) NSGAII

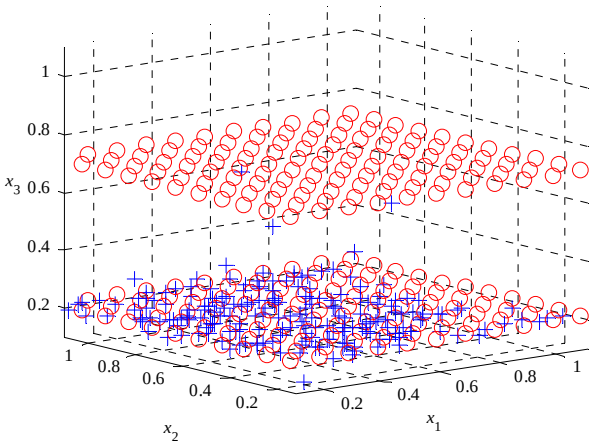

(e) SPEA2

Fig. A21. The comparison of PSs obtained by different algorithms on MMF14.

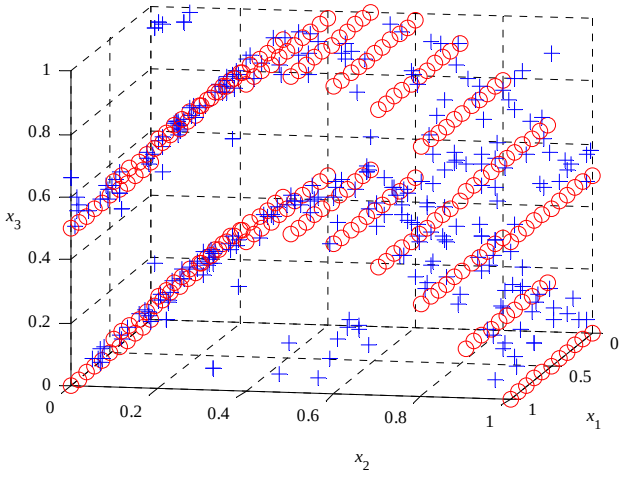

(a) MO_Ring_PSO_SCD

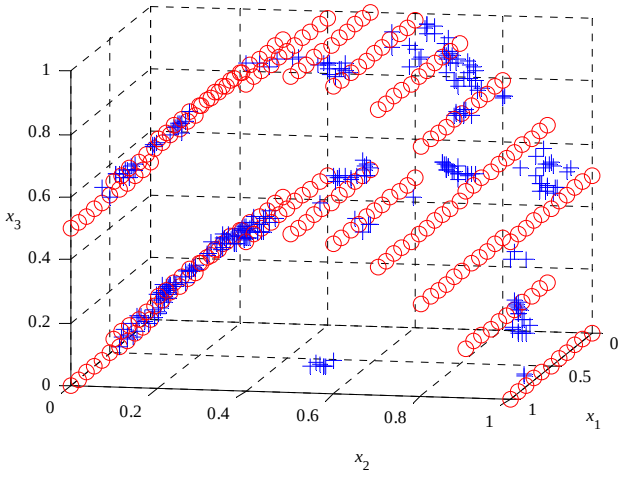

(b) DN-NSGAII

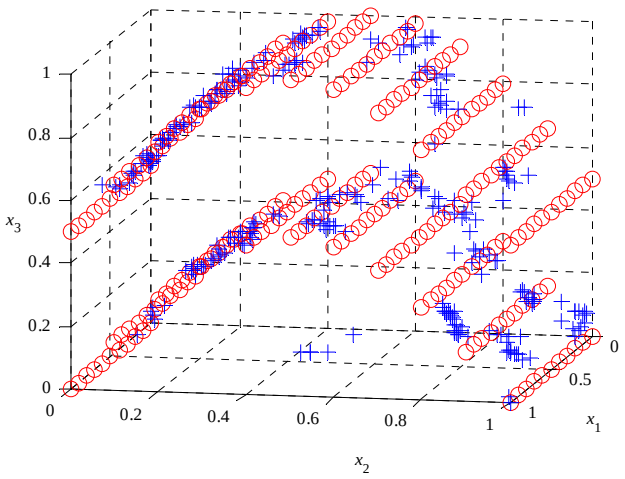

(c) Omni-optimizer

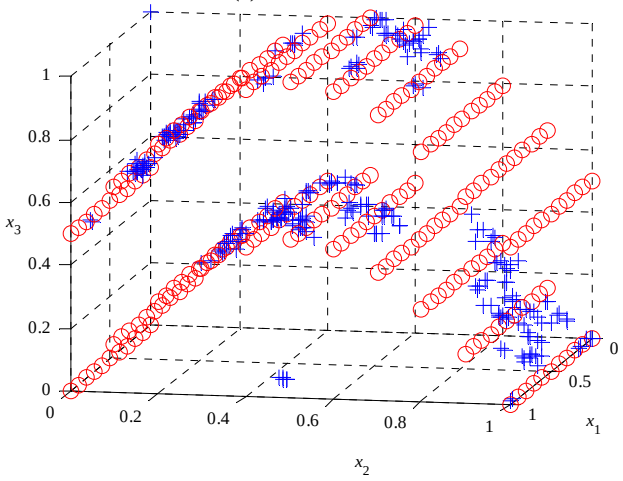

(d) NSGAII

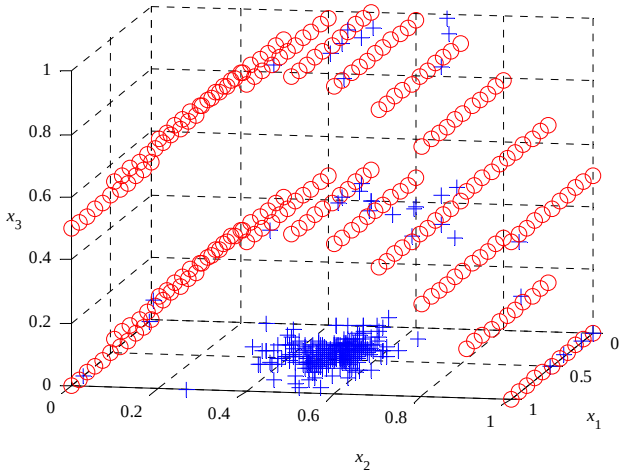

(e) SPEA2

Fig. A22. The comparison of PSs obtained by different algorithms on MMF14_a.

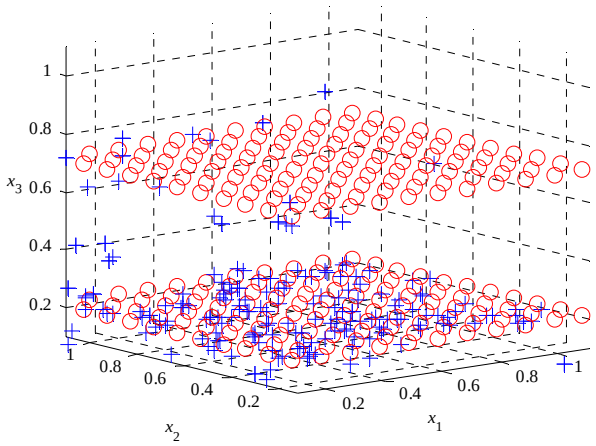

(a) MO_Ring_PSO_SCD

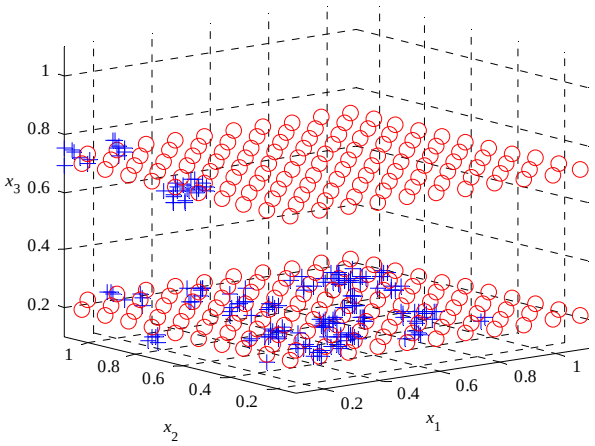

(b) DN-NSGAII

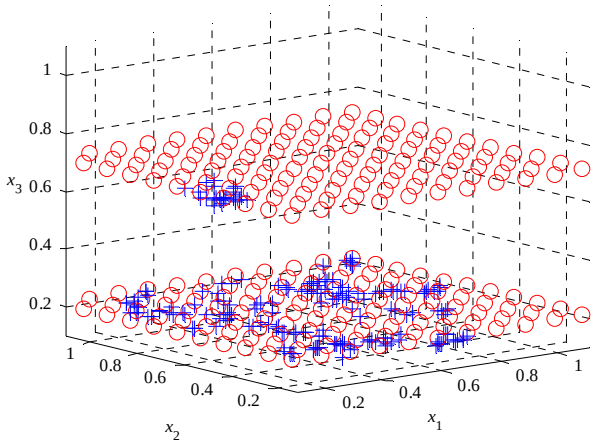

(c) Omni-optimizer

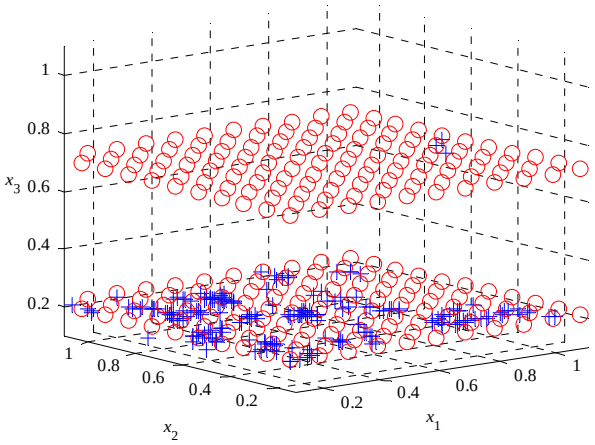

(d) NSGAII

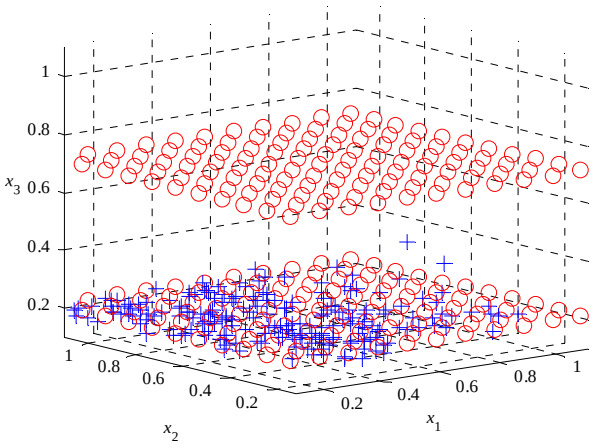

(e) SPEA2

Fig. A23. The comparison of PSs obtained by different algorithms on MMF15.

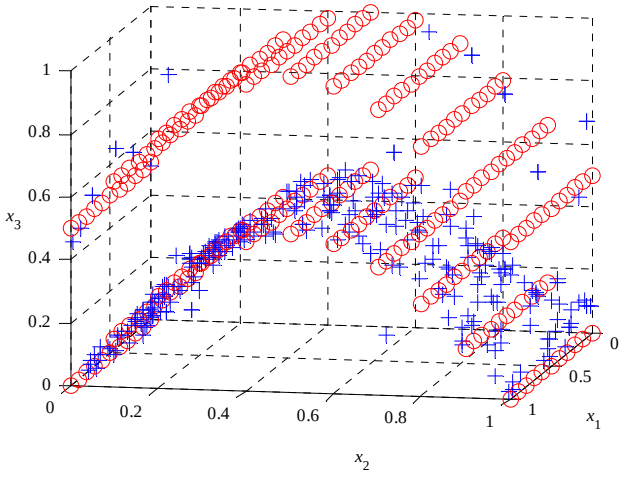

(a) MO_Ring_PSO_SCD

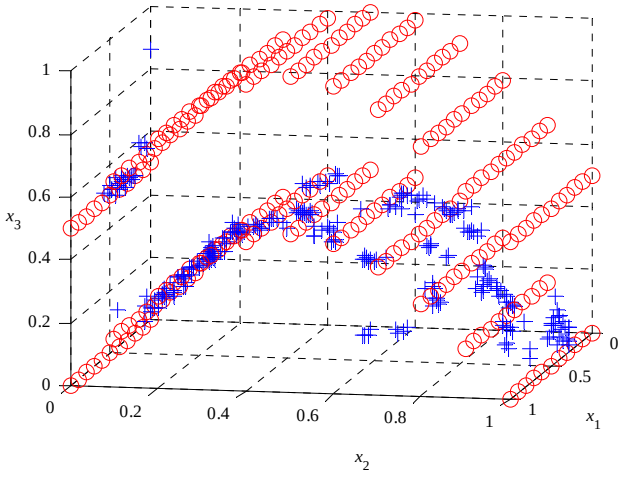

(b) DN-NSGAII

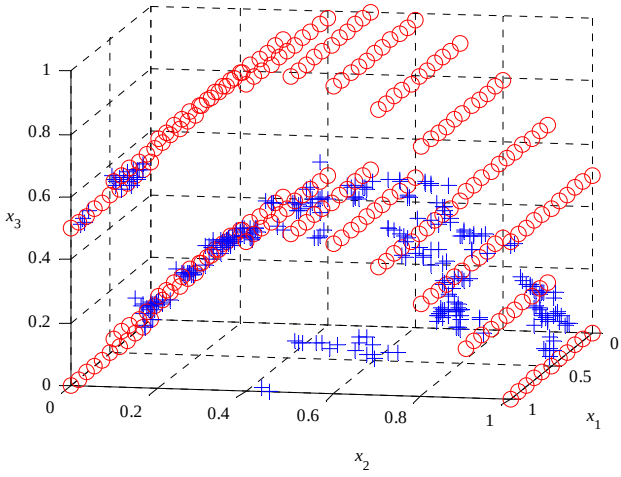

(c) Omni-optimizer

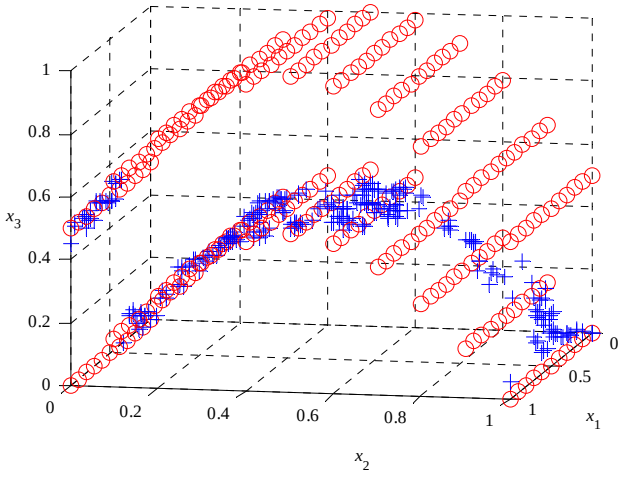

(d) NSGAII

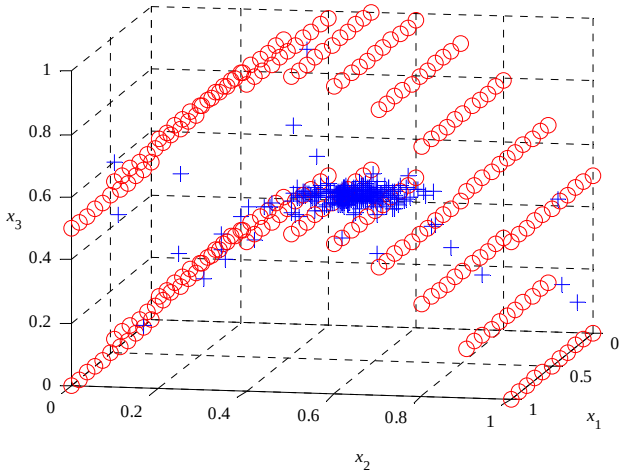

(e) SPEA2

Fig. A24. The comparison of PSs obtained by different algorithms on MMF15_a.

IV. The PFs obtained by different algorithms

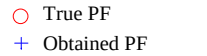

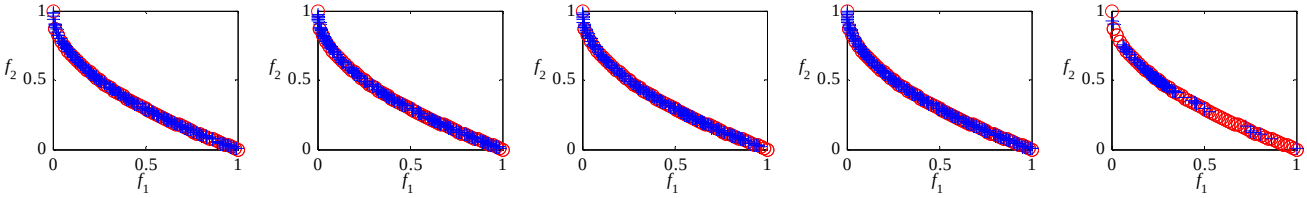

(a) MO_Ring_PSO_SCD (b) DN-NSGAII (c) Omni-optimizer (d) NSGAII (e) SPEA2

Fig. A25. The comparison of PFs obtained by different algorithms on MMF1_z.

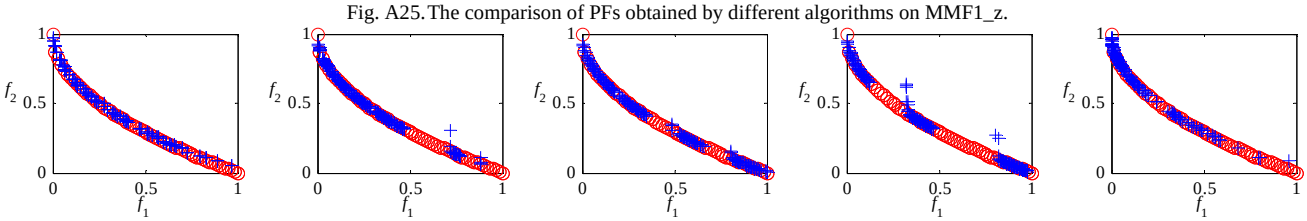

(a) MO_Ring_PSO_SCD (b) DN-NSGAII (c) Omni-optimizer (d) NSGAII (e) SPEA2

Fig. A26. The comparison of PFs obtained by different algorithms on MMF1_e.

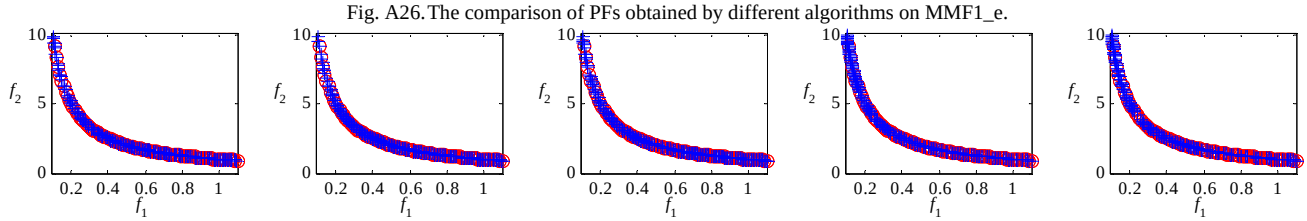

(a) MO_Ring_PSO_SCD (b) DN-NSGAII (c) Omni-optimizer (d) NSGAII (e) SPEA2

Fig. A27. The comparison of PFs obtained by different algorithms on MMF9.

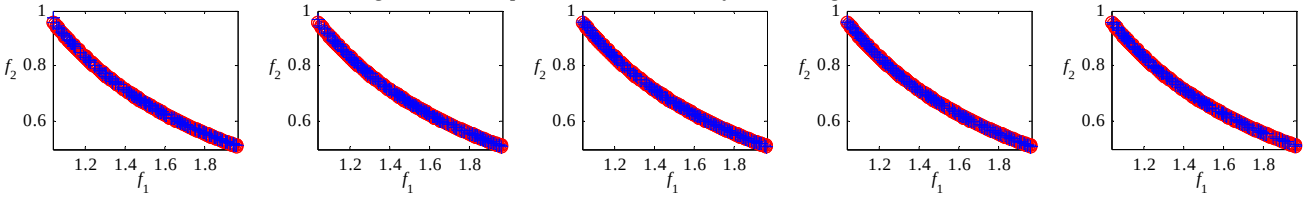

(a) MO_Ring_PSO_SCD (b) DN-NSGAII (c) Omni-optimizer (d) NSGAII (e) SPEA2

Fig. A28. The comparison of PFs obtained by different algorithms on MMF9_r.

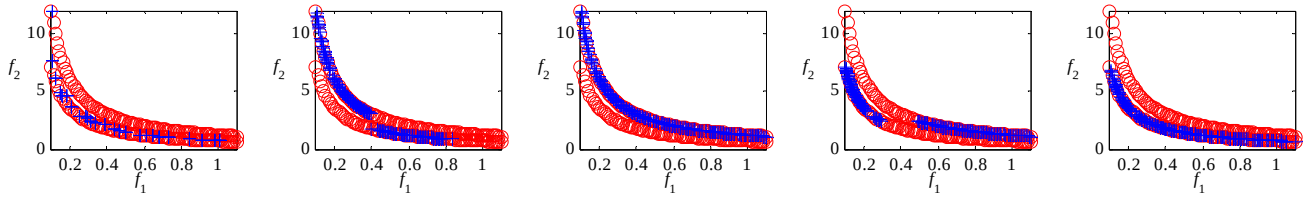

(a) MO_Ring_PSO_SCD (b) DN-NSGAII (c) Omni-optimizer (d) NSGAII (e) SPEA2

Fig. A29.The comparison of PFs obtained by different algorithms on MMF10.

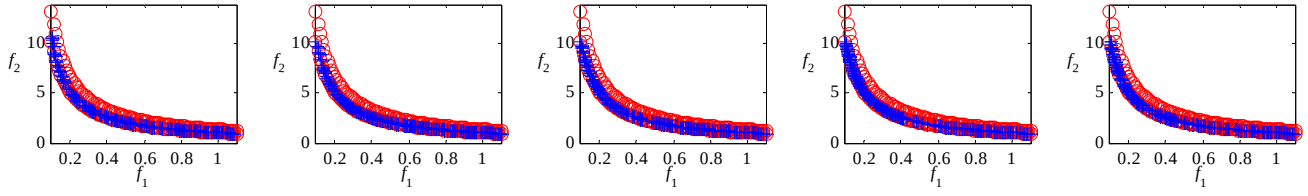

(a) MO_Ring_PSO_SCD (b) DN-NSGAII (c) Omni-optimizer (d) NSGAII (e) SPEA2

Fig. A30.The comparison of PFs obtained by different algorithms on MMF11.

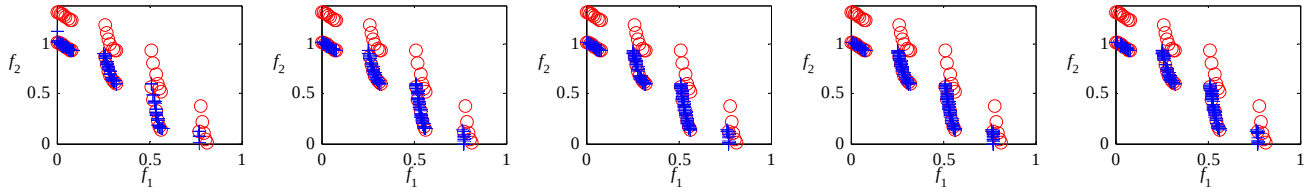

(a) MO_Ring_PSO_SCD (b) DN-NSGAII (c) Omni-optimizer (d) NSGAII (e) SPEA2

Fig. A31.The comparison of PFs obtained by different algorithms on MMF12.

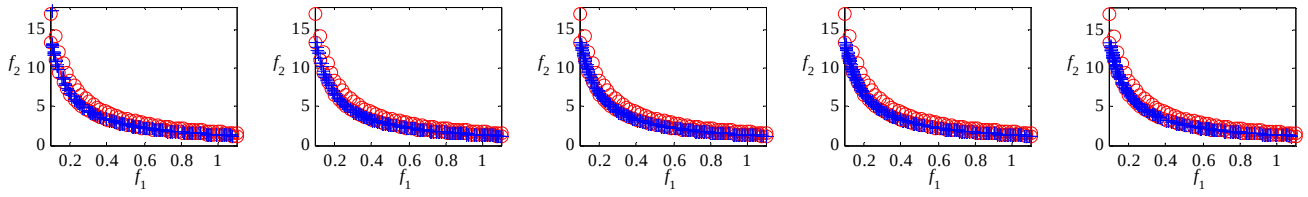

(a) MO_Ring_PSO_SCD (b) DN-NSGAII (c) Omni-optimizer (d) NSGAII (e) SPEA2

Fig. A32. The comparison of PFs obtained by different algorithms on MMF13.

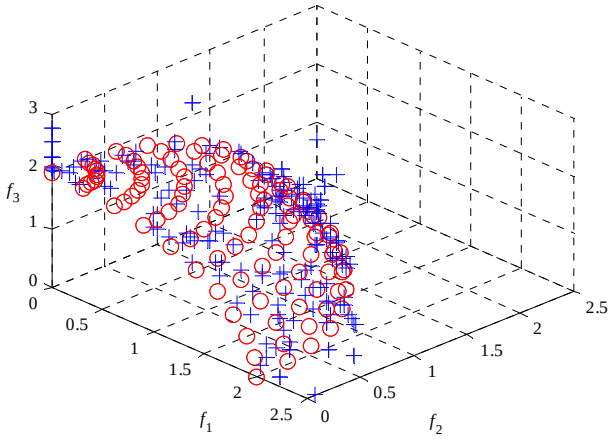

(a) MO_Ring_PSO_SCD

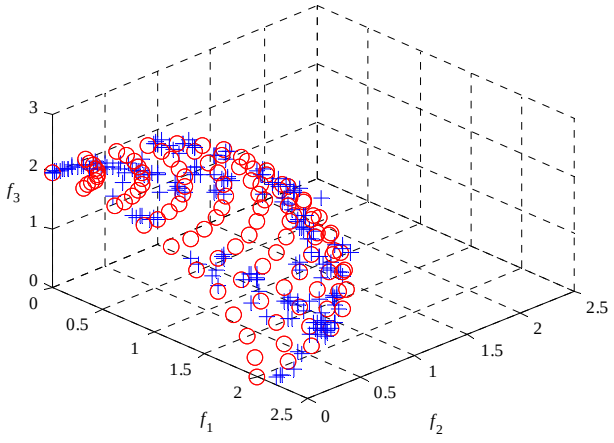

(b) DN-NSGAII

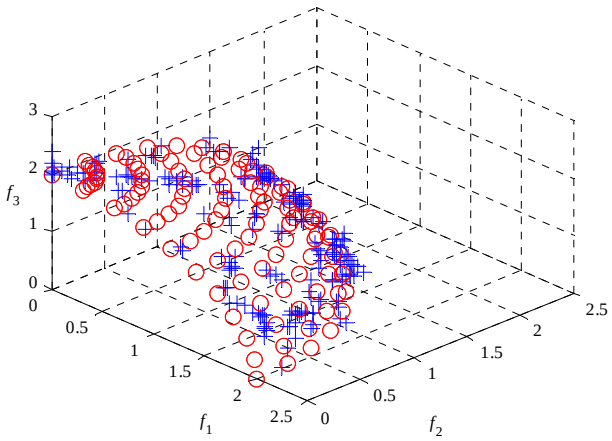

(c) Omni-optimizer

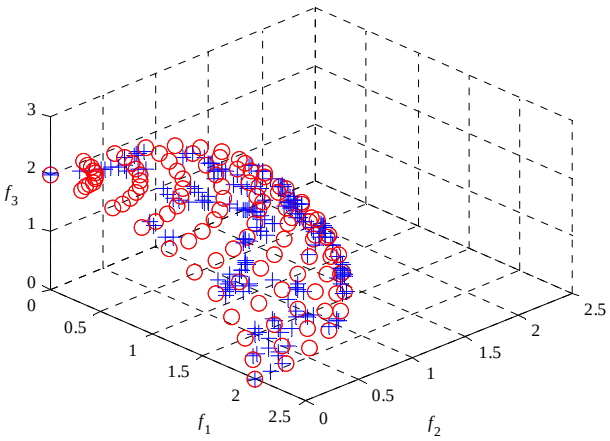

(d) NSGAII

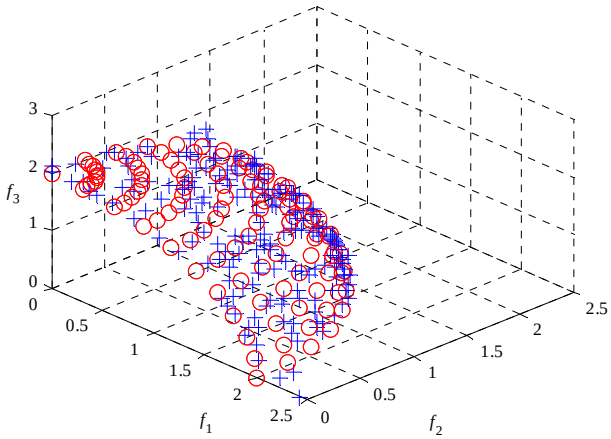

(e) SPEA2

Fig. A33. The comparison of PFs obtained by different algorithms on MMF14.

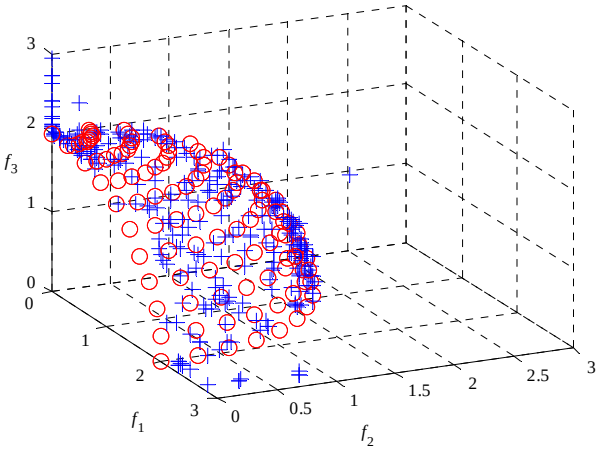

(a) MO_Ring_PSO_SCD

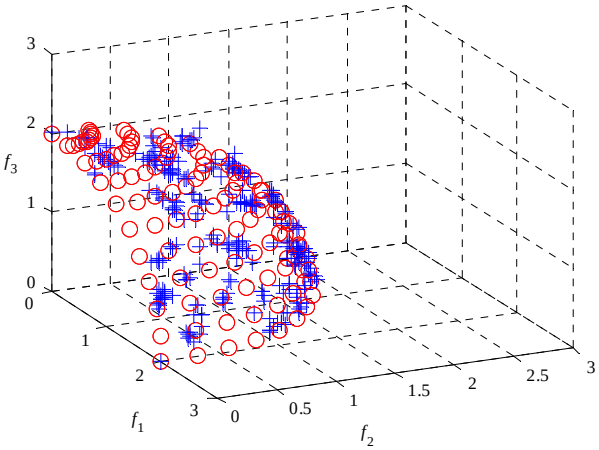

(b) DN-NSGAII

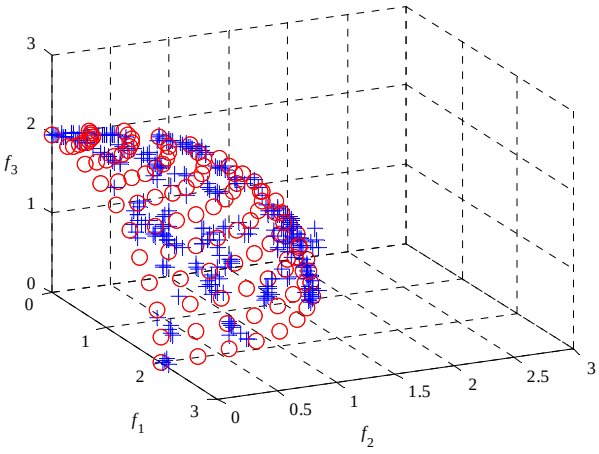

(c) Omni-optimizer

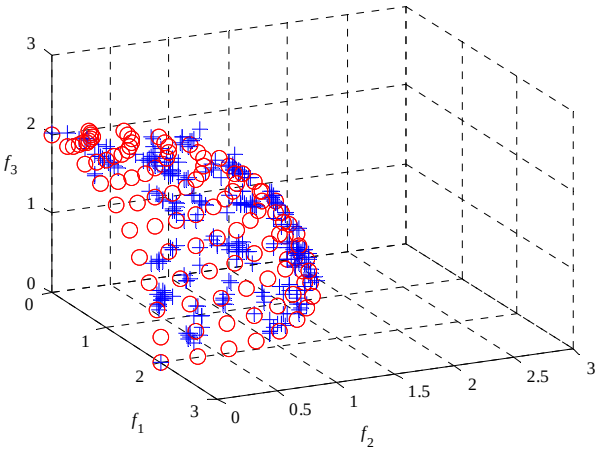

(d) NSGAII

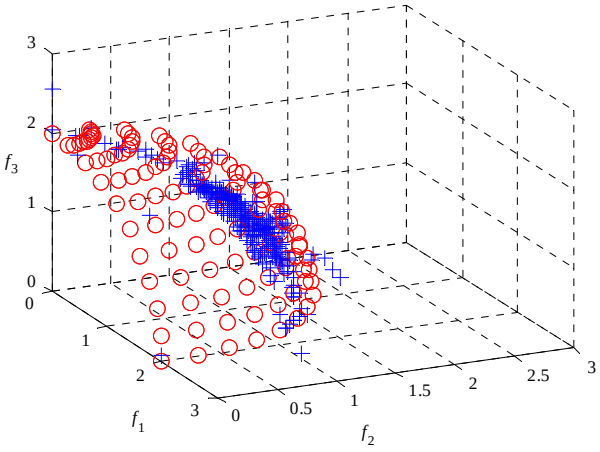

(e) SPEA2

Fig. A34. The comparison of PFs obtained by different algorithms on MMF14_a.

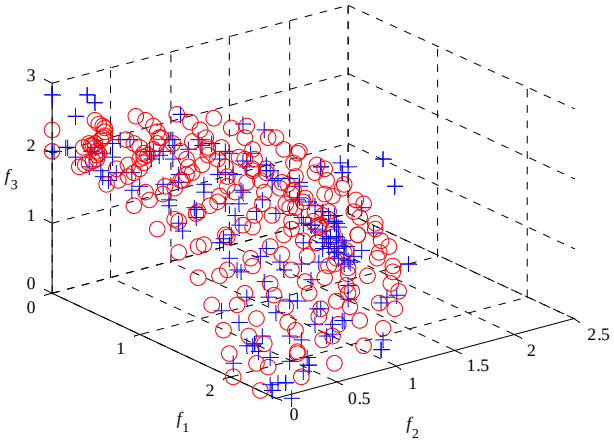

(a) MO_Ring_PSO_SCD

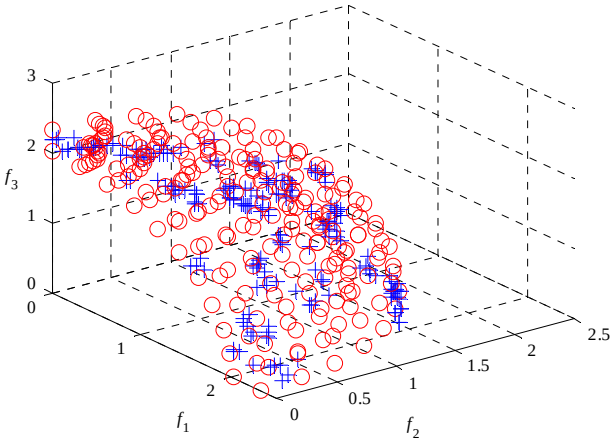

(b) DN-NSGAII

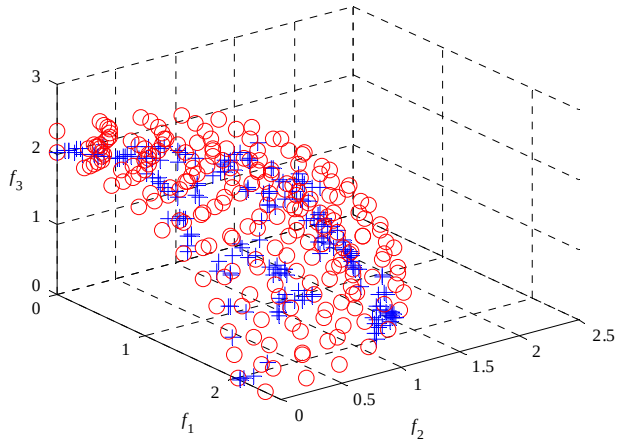

(c) Omni-optimizer

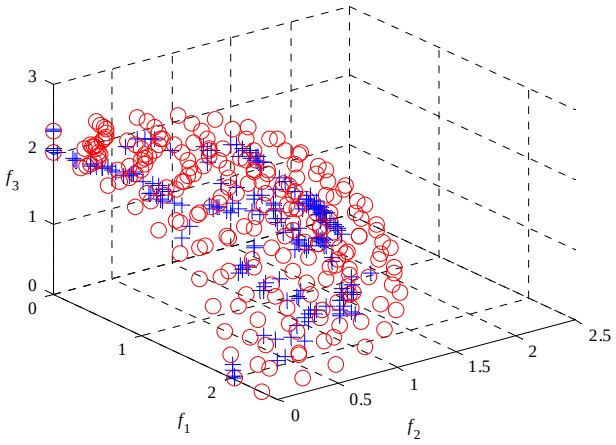

(d) NSGAII

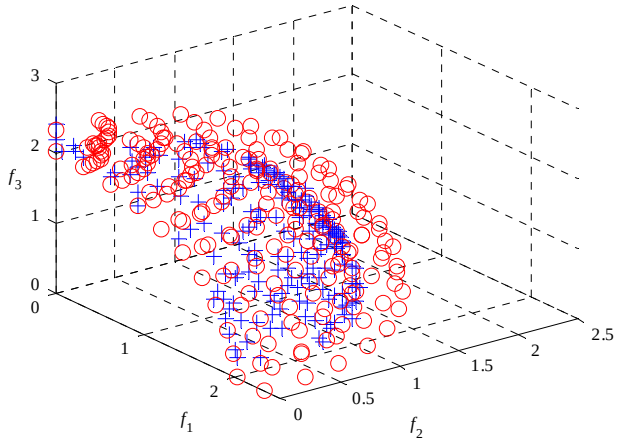

(e) SPEA2

Fig. A35. The comparison of PFs obtained by different algorithms on MMF15.

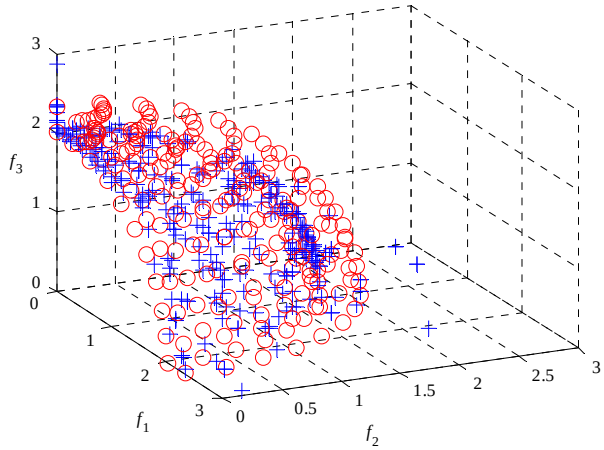

(a) MO_Ring_PSO_SCD

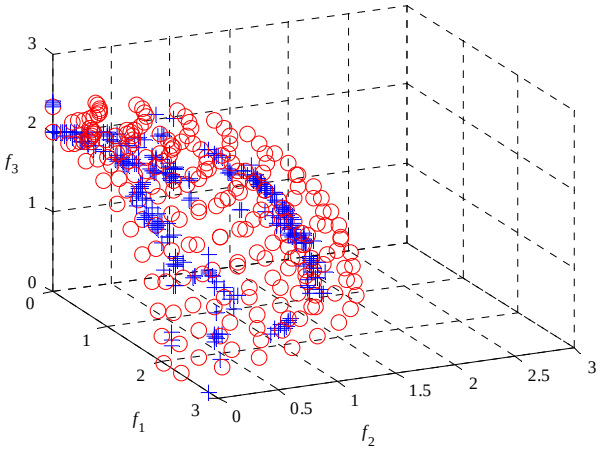

(b) DN-NSGAII

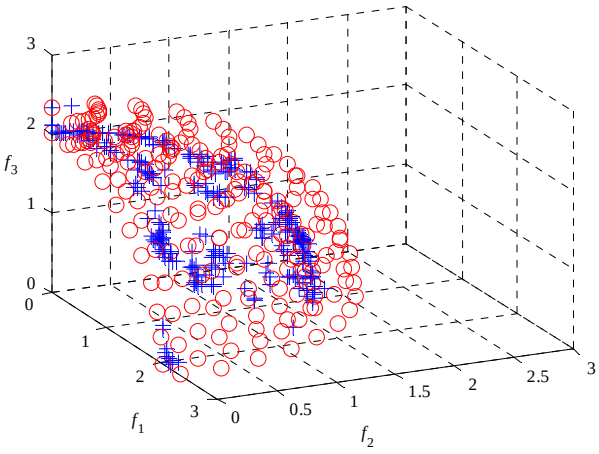

(c) Omni-optimizer

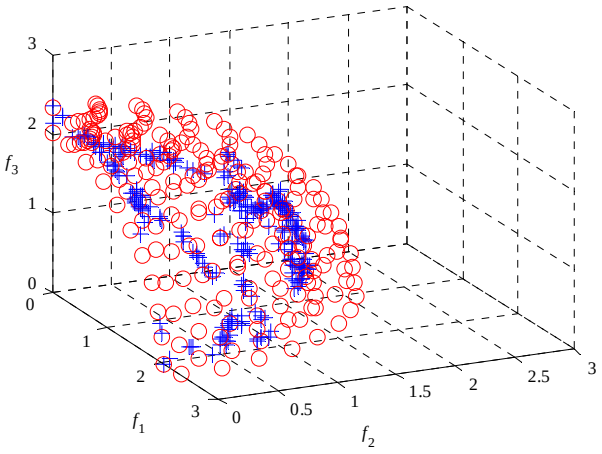

(d) NSGAII

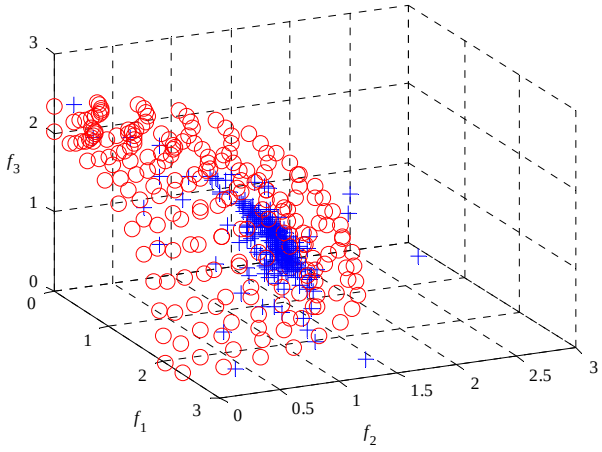

(e) SPEA2

Fig. A36. The comparison of PFs obtained by different algorithms on MMF15_a.